

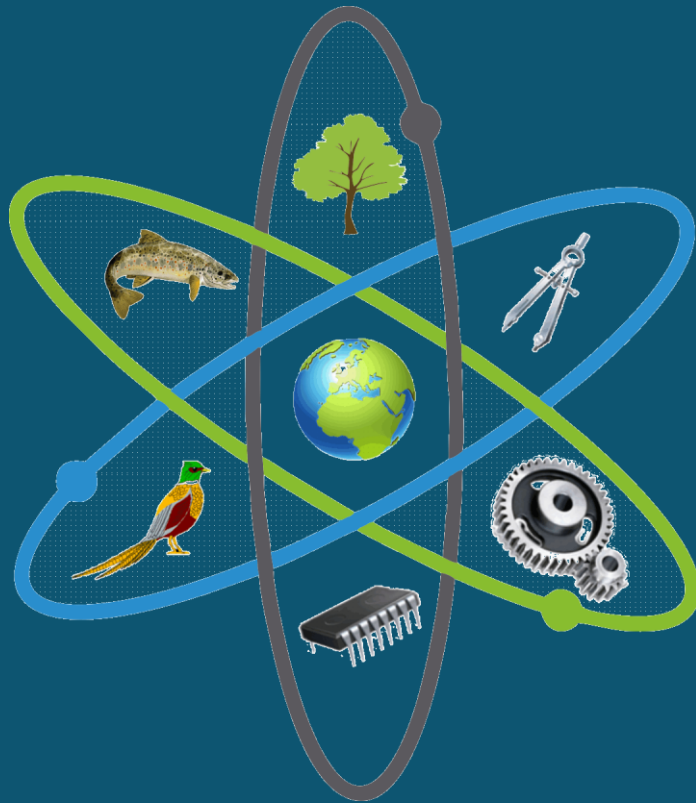
Volume: 8 Issue: 1 April - 2023

ISSN 2458-8989

NEsciences

Natural and Engineering Sciences

an International Journal



www.nesciences.com

Editor-in-Chief

Dr. Cemal Turan
Iskenderun Technical University
✉ cemal.turan@iste.edu.tr

Managing Editor

Dr. Yakup Kutlu
Iskenderun Technical University
✉ yakup.kutlu@iste.edu.tr

Editor of Natural Sciences

Dr. Servet Ahmet Dođdu
Iskenderun Technical University
✉ servet.dogdu@iste.edu.tr
Turkey

Dr. Adriana Vella
University of Malta
✉ adriana.vella@um.edu.mt
Malta

Dr. Antonia Khanaychenko
Institute of Marine Biological
Research, Sevastopol
✉ a.khanaychenko@gmail.com
Russia

Dr. Bayram Öztürk
Istanbul University
✉ ozturkb@istanbul.edu.tr
Turkey

Dr. Deniz Ergüden
Iskenderun Technical University
✉ deniz.erguden@iste.edu.tr
Turkey

Dr. Funda Turan
Iskenderun Technical University
✉ funda.turan@iste.edu.tr
Turkey

Prof. Dr. Munir H. Nayfeh
University of Illinois
✉ m-nayfeh@illinois.edu
USA

Dr. Sabina De Innocentiis
Istituti Prevenzione Ambiente ISPRA
✉ sabina.deinnoceentiis@isprambiente.it
Italy

Dr. Ali Uyan
Izmir Katip Celebi University

Editorial Board

Dr. Ahmet Gökçen
Iskenderun Technical University
✉ ahmet.gokcen@iste.edu.tr
Turkey

Dr. Athanasios Exadactylos
University of Thessaly
✉ exadact@uth.gr
Greece

Dr. Bujar Krasniqi
University of Prishtina
✉ bujar.krasniqi@uni-pr.edu
Kosovo

Dr. Deniz Yağlıođlu
Duzce University
✉ denizyaglioglu@duze.edu.tr
Turkey

Dr. Levent Bat
Sinop University
✉ leventb@sinop.edu.tr
Turkey

Dr. Nuri Basusta
Fırat University
✉ nbasusta@firat.edu.tr
Turkey

Dr. Violin Raykov
Institute of Oceanology
Bulgarian Academy of Science
✉ vio_raykov@abv.bg
Bulgaria

Technical Assistants

Dr. Serpil Karan
Iskenderun Technical University

Editor of Engineering Sciences

Dr. Tolga Depçi
Iskenderun Technical University
✉ tolga.depci@iste.edu.tr
Turkey

Dr. Alen Soldo
University of Split
✉ soldo@unist.hr
Croatia

Dr. Azza El-Ganainy
Egypt National Institute of
Oceanography and Fisheries
✉ azzaelgan@yahoo.com
Egypt

Dr. Christian Capape
Universite de Montpellier
✉ capape@univ-montp2.fr
France

Dr. Ersin Bahçeci
Iskenderun Technical University
✉ ersin.bahceci@iste.edu.tr
Turkey

Dr. Lovrenc Lipej
National Institute of Biology
✉ lovrenc.lipej@nib.si
Slovenia

Dr. Petya Ivanova
Institute of Oceanology
Bulgarian Academy of Science
✉ pavi_petya@yahoo.com
Bulgaria

Dr. Quratulan Ahmed
University of Karachi
✉ quratulanahmed_ku@yahoo.com
Turkey

Kadir Tohma
Iskenderun Technical University

Natural and Engineering Sciences

Volume 8, No: 1, April 2023

ISSN: 2458-8989

Contents

- Beta-Glycosidase Activities of Lactobacillus spp. and Bifidobacterium spp. and The Effect of Different Physiological Conditions on Enzyme Activity** 1-17
Berat Çınar Acar*, Zehranur Yüksekdağ
- BUSER Transcutaneous Electric Nerve Stimulator Device Design** 18-30
Gökhan Nur*, Büşra Nur Barış, Büşra Levent, Buse Selin Sazaklıođlu, Elvan Ak
- Parameters Response of Salt-Silicon Interactions in Wheat** 31-37
Mehmet Hanifi Akgün, Nuray Ergün*
- Capture of a Rare Smoothback Angelshark Squatina oculata (Squatinae) in Turkish Waters, with Updated Records from the eastern Mediterranean Sea** 38-45
Okan Akyol*, Tülin Çoker, H. Betül Toprak, Christian Capapé
- Morphological Description of Megalopal Stages of Three Portunid Species (Decapoda, Brachyura, Portunidae) from Indus Deltaic Area (northern-Arabian Sea)** 46-60
Urwah Inam*, Qadeer Mohammad Ali, Quratulan Ahmed, Levent Bat



Beta-Glycosidase Activities of *Lactobacillus spp.* and *Bifidobacterium spp.* and The Effect of Different Physiological Conditions on Enzyme Activity

Berat Çınar Acar * , Zehranur Yüksekdağ 

Gazi University, Faculty of Science, Department of Biology, Ankara, Türkiye

Abstract

In this research, food (cheese, yoghurt) and animal (chicken) origin 39 *Lactobacillus spp.* and human origin (newborn faeces) three *Bifidobacterium spp.* were used. To designate the β -glycosidase enzyme and specific activities of the cultures, p-nitrophenyl- β -D glikopiranozit (p-NPG) was used as a substrate. The best specific activities between *Lactobacilli* cultures were observed at *Lactobacillus rhamnosus* BAZ78 (4.500 U/mg), *L. rhamnosus* SMP6-5 (2.670 U/mg), *L. casei* LB65 (3.000 U/mg) and *L. casei* LE4 (2.000 U/mg) strains. *Bifidobacterium breve* A28 (2.670 U/mg) and *B. longum* BASO15 (2.330 U/mg) strains belonging to the *Bifidobacterium* cultures had the highest specific activity capabilities. Optimization studies were performed to designate the impact of different pH, temperature, and carbon sources on the β -glucosidase enzyme of *L. rhamnosus* BAZ78 strain (β -Glu-BAZ78), which exhibits high specific activity. As optimum conditions, pH was detected as 7.5, the temperature as 30° C, and the carbon source as 2% glucose for the enzyme. Although the enzyme activity changed as the physiological conditions changed, the β -Glu-BAZ78 showed the highest specificity in the control groups.

Keywords:

Lactobacillus, *Bifidobacterium*, β -glycosidase enzyme activity, probiotic, optimization

Article history:

Received 08 September 2022, Accepted 11 December 2022, Available online 10 April 2023

Introduction

Bifidobacterium spp. is a widespread inhabitant of the human intestinal system during life (Modrackova et al., 2020). Gram-positive lactobacilli are in the Lactic acid bacteria (LAB) group and are outstanding constituents of the intestinal microbiome. Due to their useful health impacts,

*Corresponding Author: Berat ÇINAR ACAR, E-mail: beratcinar@gazi.edu.tr

lactobacilli and bifidobacteria are used as probiotics and accepted GRAS (generally regarded as safe), which means they are secure when used properly (Naidu et al., 1999; Garbacz, 2022). Beneficial bacteria that can enhance the microbial environment of the intestinal system, arrange immune-concerned genes and augment resistance to pathogens are called probiotics (Kumar et al., 2017; Meng et al., 2017; Gao et al., 2018). Some inhibitory substances produced by lactic acid bacteria and bifidobacteria have beneficial effects on health such as inhibiting the growth of pathogenic microorganisms in the gastrointestinal tract, playing a role in regulating the immune system, maintaining their vitality in the gastrointestinal tract, and having the ability to grow at low pH values and with bile salts in a wide temperature range. Therefore, they are used as probiotics (Gao et al., 2018; Zhu et al., 2022). In addition, these bacteria are used as human probiotics because of their useful contribution effects such as improving the intestinal microbiota, preventing diarrhoea (Maldonado et al., 2019), strengthening the immune system, lowering the cholesterol level in the blood, improving lactose digestibility, facilitating calcium absorption (O'Callaghan ve van Sinderen, 2016), suppressing cancer cells (Garbacz, 2022), strengthening mineral absorption, and sticking to the intestinal mucosa (Dupont et al., 2014, Kosmerl et al., 2021).

Polysaccharides (especially cellulose) are compounds that are abundant in the biosphere and constitute an important source of recyclable chemicals and fuels. A cellulase enzyme complex secreted by cellulolytic organisms can hydrolyze cellulose to glucose. The enzyme complex includes three enzymes: endoglucanase, cellobiohydrolases, and β -glucosidase (Zang et al., 2018; Ariaeenejad et al., 2020). Endoglucanases break off the inner β -1,4-glycosidic bonds of cellulose by hydrolysis to form new chain ends, and exoglucanases form soluble cellobiose units by cutting these new cellulose chains formed at the ends (Teugjas & Våljamäe, 2013; Pang et al., 2017). The enzyme β -glucosidase, which is responsible for the hydrolysis of cellulose, has been the focus of many studies because cellulose is the amplest substrate on earth and an essential renewable energy source in the future (Kara et al., 2011; Tamaki et al., 2016; Seidel & Lee, 2020). β -Glucosidases are a heterogeneous group of hydrolytic enzymes. This enzyme plays a crucial role in various biological activities like cellular signalling, biosynthesis and degradation of structural and storage polysaccharides, and host-pathogen interactions (Singh et al., 2016; Zang et al., 2018).

β -Glucosidases are extensively used in different processes like the hydrolysis of isoflavone glycosides, the generation of fuel ethanol from agricultural residues, and the dismissal of aromatic compounds from unwanted precursors (Singhania et al., 2013; Chen et al., 2021). β -Glucosidases could be generated by several organisms, such as fungi (*Aspergillus niger*, *Penicillium decumbens*), yeasts (*Candida spp.*) archaea, and a few bacteria (Singh et al., 2016; Zang et al., 2018; Chen et al., 2021). Also, plants can accumulate β -glucosides and β -glucosinolates in their bodies and release them into the environment when needed. β -glucosidic substrates and β -glucosidases are stockpiled in different substructures or tissue sections of the cell. As a result of damage to the cell when pathogens or herbivores come to plant tissues, the substrate and the enzyme combine. At this time, the hydrolysis of the substrates begins and the aglycons or other degradation products released as

a result of hydrolysis create a toxic effect and prevent the entry and dispersal of harmful organisms to the plants. Thus, β -glucosidase enzymes play a significant role in the defence system against plant pests. β -glucosidases are highly effective in improving the quality of wine, tea, and fruit juice. Aglycones are structures that are highly effective in food quality and production. However, aglycones must be hydrolyzed by β -glucosidase enzymes to form. When the β -glucosidase enzyme is added during or after production, an increase is observed in the taste, flavour, aroma, and other quality factors of the products (Grohmann et al., 1999; Sener, 2015).

In this research, it was aimed to detect β -glucosidase enzyme activities with p-nitrophenyl- β -D glycopyranoside (p-NPG) substrate of *Lactobacillus* and *Bifidobacterium* strains isolated from various sources. Optimization studies of enzyme activities of *L. rhamnosus* BAZ78 strain showing high specific activity at different pH, temperature, and carbon sources were also aimed at.

Materials and Methods

In this study, 39 *Lactobacillus* spp. (*L. casei* (13), *L. acidophilus* (11), *L. rhamnosus* (4), *L. delbrueckii* subsp. *delbrueckii* (3), *L. brevis* (1), *L. paracasei* subsp. *paracasei* (1), *L. delbrueckii* subsp. *bulgaricus* (1), *Ligilactobacillus salivarius* (3), *Limosilactobacillus fermentum* (2)), human (17), food (4) and animal (18) origin, and 3 *Bifidobacterium* spp. (*B. breve* (2) and *B. longum* (1)) strains, isolated from newborn faeces, were used. The strains were obtained from the Gazi University Faculty of Science Biotechnology Laboratory Culture Collection.

Man & Rogosa and Sharp (MRS) medium was used to encourage the growth of lactobacilli and the determination of β -glucosidase enzyme activities. To determine the effect of media used in enzyme optimization studies on enzyme activity, 2% sucrose, lactose, fructose, and cellobiose added media were used instead of glucose in the MRS medium. Trypticase Phytone Yeast Extract medium (TPY) was used to encourage the growth of bifidobacteria cultures and to determine β -glucosidase activities, and Man & Rogosa and Sharp medium with Modified Cysteine (MMRSC) and Man & Rogosa and Sharp medium with Cysteine (MRSC) were used for enzyme optimization studies. In addition, all experimental studies with bifidobacteria were carried out using an anaerobic kit (Oxoid, Anaerobic generating kit), which provides 10% CO₂ release to the environment in the anaerobic jar (Oxoid, Anaerojar).

Determination of B-Glucosidase Activities of Strains

To designate the enzyme activities of the bacterial cultures, after the cultures were developed in the appropriate medium, they were centrifuged at 5000 rpm for 20 min at 4°C (Sigma 2-16 KC). Cell pellet and supernatant were separately washed twice with 0.5 M potassium phosphate buffer (PBS) (0.02% KCl, 0.144% Na₂HPO₄, 0.8% NaCl, 0.024% KH₂PO₄, pH 7.0) and their optical densities were adjusted to Mc Farland 5 (~ 15 log cfu/mL). To break down the cell wall of bacteria, the samples were kept for 5 min in an ultrasonication device (Vibra-Cell, Sonics & Materials Inc.

Danbury, CT USA brand) tuned to 50 MHz frequency and ice was added. Centrifugation was applied at 1000 rpm for 10 min at 4°C to precipitate cell wastes. For the measurement of β -glucosidase activity, p-NPG was used as a substrate (Strahsburger et al., 2017). Then 0.5 mL of the cell suspension was added to the mixture containing 2 mL 2.5 mM p-NPG in 0.5 M PBS (pH 7.5), and the mixture was incubated for 30 min at 30°C. The reaction was stopped by keeping it at 95°C for 5 min. The β -glucosidase activities of the cultures were detected by measuring at a wavelength of 420 nm in a spectrophotometer (Hitachi UV-1800, Japan) (Choi, 2002). It was prepared by using 1 mL of 0.5 M PBS (pH 7.5) instead of the crude extract as a blind.

One unit of β -glucosidase enzyme is the amount of enzyme that catalyzes the formation of 1 μ mol of product per minute or the conversion of 1 μ mol of the substrate ($U = \mu\text{mol}/\text{min}$). The specific activity of an enzyme is the number of enzyme units per 1 mg of protein. The β -glucosidase enzyme activity of the cultures was calculated using the Beer-Lambert law as stated below (Temizkan et al., 2008).

$$\text{Enzyme unit in the sample} = (V_t \times dA/dt \times 1000 \times \text{dilution factor}) / (\epsilon \lambda \times v_s \times d) = (U/L)$$

dA/dt : Change in absorbance per unit time (minute) (min^{-1})

$\epsilon \lambda$: Absorption coefficient ($\text{cm}^2 \text{mol}^{-1}$)

d : The light path of the cuvette (usually 1 cm)

V_t : Total volume of the reaction mixture (mL)

v_s : Volume of the sample (enzyme) involved in the reaction (mL)

$$\text{Specific Activity (U/mg)} = (\text{Enzyme activity (U/mL)}) / (\text{Protein amount (mg/mL)})$$

Moreover, the relative activity of the strain with the highest specific activity was calculated according to the below formula (Yüksekdağ & Yüksekdağ, 2021).

Relative activity (%) = (Investigated parameter's enzyme activity/Enzyme activity at optimum conditions) x 100.

The Effect of Different Physiological Conditions on the B-Glucosidase Enzyme

L. rhamnosus BAZ78 strain, which showed the highest specific activity, was selected from the cultures whose β -glucosidase activities were determined, and enzyme optimization studies were carried out at different pH, temperature, and carbon sources. To determine the activities at different pHs, the pH of 0.5 M PBS was adjusted to 4.0, 5.0, 6.0, 7.0, 7.5 (control), and 8.0 using 3 M HCl and 3 M NaOH. After adding 0.5 mL of the cell suspension to the mixture including 2 mL 2.5 mM p-NPG in 0.5 M PBS (pH 7.5), the mixture was mixed at different temperatures (30°C-control,

37°C, 40°C, 50°C, and 60°C) and the impact of temperature on the activity was designated by measuring the enzyme activity of the mixture, which was left to incubate at different temperature values. To specify the β -glucosidase activities of the samples in different carbon sources, instead of 2% glucose (control), fructose, sucrose, lactose, and cellobiose were added into MRS broth, which is the most suitable carbon source for the development of BAZ78.

Statistical Analysis

All studies were carried out in three parallels and three replications and the average results of the studies were given. The data obtained were analyzed using the SPSSe statistical software (IBM SPSS Statistics Data Editor, version 22). With the Pearson correlation, it was investigated whether there was a correlation between the enzyme activity-protein amount and protein amount-specific activities of the strains.

Results

Due to their probiotic properties, lactobacilli and bifidobacteria could be an alternative to plants as a source of β -Glucosidase enzyme, which has a very different commercial use potential. For this reason, this study, it was aimed to investigate safe and new lactobacilli and bifidobacteria with high enzyme activity.

B-Glucosidase Enzyme Activity

Strains belonging to *Lactobacillus* and *Bifidobacterium* genera formed a product (p-nitrophenol) with their β -glucosidase enzyme activities by using p-NPG to be a substrate. Product formation was seen when the mixture containing p-NPG turned yellow. β -glucosidase enzyme activities, protein amounts, and specific activities observed in the pellets of the cultures are given in Table 1.

Among the cultures belonging to the genus *Lactobacillus*, the highest specific activity was in *L. rhamnosus* BAZ78 (4.500 U/mg), and the lowest specific activity was in *L. delbrueckii* subsp. *delbrueckii* ZYN31 (0.250 U/mg). It was determined that *B. breve* A28 (2.670 U/mg) and *B. longum* BASO15 (2.330 U/mg) strains had the highest specific activity ability among the cultures belonging to the *Bifidobacterium* genus (Table 1). When the specific activities of the bacteria were evaluated, significant differences in activity were observed between strains in both species ($p < 0.01$).

Table 1. The lowest and highest values of the β -glycosidase enzyme, specific enzyme activity, and protein content of *Lactobacilli* and *Bifidobacteria*

<i>Bacteria</i>	<i>Protein content</i> (mg/mL)	<i>Enzyme activity</i> (U/mL)	<i>Specific activity</i> (U/mg)
<i>L. acidophilus</i> BAZ54	0.050±0.003	0.050±0.001	1.000±0.001
<i>L. acidophilus</i> BAZ51	0.020±0.006	0.010±0.002	0.500±0.007
<i>L. acidophilus</i> BAZ59	0.030±0.002	0.010±0.001	0.330±0.001
<i>L. acidophilus</i> BAZ63	0.020±0.001	0.020±0.000	1.000±0.000
<i>L. acidophilus</i> BAZ29	0.040±0.006	0.020±0.001	0.500±0.001
<i>L. acidophilus</i> BAZ43	0.020±0.005	0.010±0.002	0.500±0.003
<i>L. acidophilus</i> BAZ22	0.020±0.004	0.010±0.002	0.500±0.001
<i>L. acidophilus</i> BAZ61	0.050±0.001	0.020±0.003	0.400±0.001
<i>L. acidophilus</i> BAZ36	0.040±0.001	0.020±0.000	0.500±0.000
<i>L. acidophilus</i> ZYN13	0.060±0.006	0.020±0.001	0.330±0.004
<i>L. acidophilus</i> ACS6	0.040±0.003	0.070±0.005	1.750±0.002
<i>L. casei</i> LB65	0.010±0.001	0.030±0.001	3.000±0.001
<i>L. casei</i> LB68	0.060±0.001	0.080±0.000	1.330±0.000
<i>L. casei</i> LE4	0.028±0.001	0.056±0.001	2.000±0.001
<i>L. casei</i> LE7	0.060±0.001	0.080±0.001	1.330±0.002
<i>L. casei</i> LB17	0.110±0.001	0.090±0.000	0.820±0.000
<i>L. casei</i> LB19	0.060±0.002	0.080±0.001	1.330±0.005
<i>L. casei</i> LB6	0.080±0.001	0.070±0.001	0.880±0.001
<i>L. casei</i> LB23	0.070±0.001	0.060±0.001	0.860±0.001
<i>L. casei</i> LB49	0.080±0.001	0.070±0.001	0.880±0.001
<i>L. casei</i> LB61	0.080±0.003	0.060±0.001	0.750±0.002
<i>L. casei</i> LB83	0.060±0.000	0.080±0.000	1.330±0.000
<i>L. casei</i> LB74	0.090±0.001	0.090±0.009	1.000±0.008
<i>L. casei</i> LB64	0.070±0.002	0.050±0.001	0.710±0.001
<i>L. rhamnosus</i> GD11	0.070±0.001	0.080±0.005	1.140±0.002
<i>L. rhamnosus</i> LP2	0.060±0.001	0.060±0.007	1.000±0.002
<i>L. rhamnosus</i> BAZ78	0.006±0.001	0.027±0.002	4.500±0.002
<i>L. rhamnosus</i> SMP6-5	0.026±0.001	0.069±0.001	2.670±0.001
<i>L. salivarius</i> ZYN9	0.020±0.001	0.030±0.000	1.500±0.000
<i>L. salivarius</i> ZYN15	0.120±0.001	0.050±0.002	0.420±0.001
<i>L. salivarius</i> ZYN23	0.080±0.01	0.040±0.000	0.500±0.000
<i>L. delbrueckii subsp. delbrueckii</i> ZYN33	0.020±0.002	0.020±0.001	1.000±0.001
<i>L. delbrueckii subsp. delbrueckii</i> ZYN31	0.040±0.001	0.010±0.001	0.250±0.001
<i>L. delbrueckii subsp. delbrueckii</i> BAZ32	0.020±0.001	0.010±0.003	0.500±0.002
<i>L. fermentum</i> ZYN17	0.030±0.001	0.020±0.001	0.670±0.001
<i>L. fermentum</i> LB16	0.090±0.001	0.070±0.000	0.780±0.000
<i>L. brevis</i> LB63	0.080±0.002	0.050±0.001	1.600±0.001
<i>L. delbrueckii subsp. bulgaricus</i> B3	0.110±0.001	0.050±0.005	0.450±0.003
<i>L. paracasei subsp. paracasei</i> BKS20	0.050±0.001	0.080±0.000	1.600±0.000
<i>B. breve</i> A26	0.050±0.000	0.060±0.000	1.200±0.000
<i>B. breve</i> A28	0.027±0.000	0.072±0.000	2.670±0.000
<i>B. longum</i> BASO15	0.030±0.005	0.070±0.000	2.330±0.000

The Effect of Different Physiological Conditions on Enzyme Activity

L. rhamnosus BAZ78 strain with the highest specific activity was selected for use in enzyme optimization (pH, temperature, and carbon source) studies. Enzyme activities, specific activities, and protein amounts were determined by using 0.5 M PBS adjusted to various pH values (4.0, 5.0, 6.0, 7.0, 7.5, and 8.0) of the *L. rhamnosus* BAZ78 strain (Table 2).

Table 2. Effect of pH, temperature and media on the β -glycosidase enzyme, specific enzyme activity, and protein content in *Lactobacillus rhamnosus* BAZ78 strain

	pH					
	4.0	5.0	6.0	7.0	7.5 (Control)	8.0
Protein content (mg/mL)	0.010±0.001	0.008±0.001	0.005±0.003	0.006±0.001	0.006±0.002	0.007±0.001
Enzyme activity (U/mL)	0.014±0.007	0.014±0.001	0.017±0.010	0.024±0.005	0.027±0.004	0.014±0.010
Specific activity (U/mg)	1.400±0.007	1.800±0.001	3.400±0.005	4.000±0.001	4.500±0.002	2.000±0.009
	Temperature (° C)					
	30 (Control)	37	40	50	60	
Protein content (mg/mL)	0.006±0.002	0.006±0.000	0.007±0.002	0.009±0.002	0.010±0.001	
Enzyme activity (U/mL)	0.027±0.004	0.021±0.000	0.018±0.003	0.020±0.005	0.018±0.001	
Specific activity (U/mg)	4.500±0.002	3.500±0.000	2.570±0.002	2.220±0.003	1.800±0.001	
	Carbon Sources					
	Glucose (Control)	Fructose	Lactose	Sucrose	Cellobiose	
Protein content (mg/mL)	0.006±0.002	0.025±0.001	0.032±0.001	0.028±0.001	0.030±0.001	
Enzyme activity (U/mL)	0.027±0.004	0.040±0.001	0.041±0.003	0.032±0.005	0.036±0.001	
Specific activity (U/mg)	4.500±0.002	1.600±0.001	1.280±0.003	1.143±0.005	1.200±0.001	

The protein amount of the β -Glu-BAZ78 at different pH values was determined as 0.005-0.010 mg/mL, β -glucosidase enzyme activity as 0.014-0.027 U/mL, and specific activity as 1.400-4.500 U/mg. It was observed that the β -Glu-BAZ78 did not lose its activity at different levels of pH, and the specific activity was the best at pH 7.5 and the lowest at pH 4.0 (Figure 1).

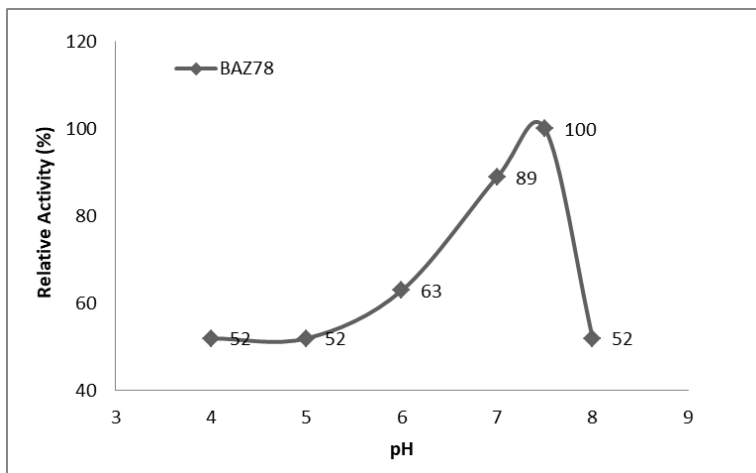


Figure 1. Effect of pH on β -glucosidase enzyme

The mixture containing 2 mL 2.5 mM of p-NPG, in 0.5 M potassium phosphate buffer (pH 7.5) was added to 0.5 mL of the BAZ 78 cell suspension. The mixture was then incubated at different temperatures (30° C, 37° C, 40° C, 50° C, and 60° C). The impacts of different temperatures on the enzyme activity are given in Table 2. The protein amount of the β -Glu-BAZ78 was designated as 0.006-0.010 mg/mL, enzyme activity was detected as 0.018-0.027 U/mL, and specific activity was 1.800-4.500 U/mg at varying temperature values. The optimum temperature of the β -Glu-BAZ78 was found to be 30° C (Figure 2).

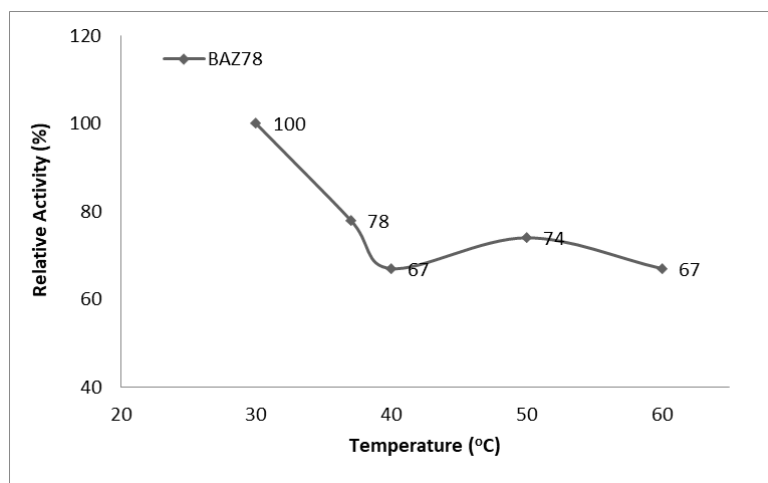


Figure 2. Effect of temperature on β -glucosidase enzyme

The specific activities, enzyme activities, and protein amounts of the strains were determined by using different carbon sources (lactose, sucrose, fructose, cellobiose) at the same rate instead of 2% glucose in the MRS medium in which the *L. rhamnosus* BAZ78 strain was developed (Table 2). The protein amount of the enzyme in different carbon source MRS medium of BAZ78 strain was determined as 0.006-0.032 mg/mL, enzyme activity as 0.027-0.041 U/mL, and specific activity as 1.143-4.500 U/mg. It was detected that the most suitable carbon source for the β -Glu-BAZ78 was MRS medium containing 2% glucose. The lowest specific activity was observed in the medium containing 2% sucrose (Figure 3).

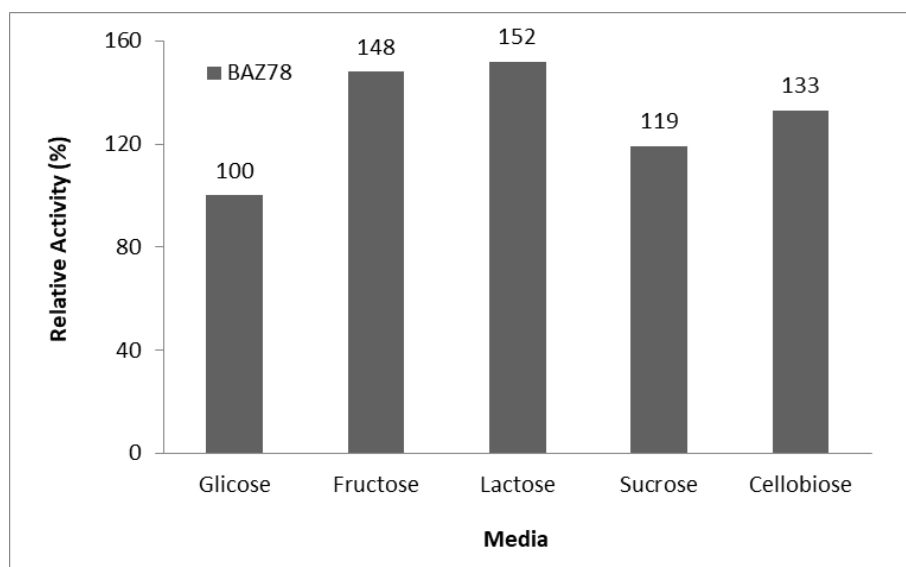


Figure 3. Effect of different media on β -glucosidase enzyme

Discussion

Isoflavones are present as the forms of glycosides and aglycones. The high content of isoflavones exists in glycoside forms but the biological activity of isoflavones is primarily from aglycones. Thus, it is important and necessary to transform isoflavone glycosides into the aglycones form (Lu et al., 2022). The β -glucosidase enzyme is a substantial enzyme that could convert the glucoside form of isoflavone to the aglycone form, which is beneficial for health and generated by microorganisms. Although the β -glucosidase enzyme is more common in plants, moulds, and yeasts, it can be generated by lactic acid bacteria and bifidobacteria (Esteve-Zarzoso et al., 1998; Marazza et al., 2009; Yüksekdağ et al., 2018).

In this research, the β -Glucosidase enzyme activity of *Lactobacillus* and *Bifidobacterium* bacteria was investigated. Since the β -Glucosidase enzyme is an intracellular enzyme (Marazza et al., 2009; Yüksekdağ et al., 2018; Huang et al., 2021; Lenz et al., 2022), ultrasonication, which is widely used as a mechanical method, was used to break down the cell wall of bacteria in enzyme extraction in our study (Carević vd., 2015). To support the intracellular β -glucosidase enzyme

activity of 42 strains belonging to 39 lactobacilli and 3 bifidobacteria cultures, the enzyme activity was also examined in the culture supernatants. No enzyme activity was found in the culture supernatants. Forty-two strains isolated from different sources (human, food, animal) were used, and differences in enzyme activities (Table 1) were observed according to the isolation source. In general, when the specific activities of the strains are evaluated, it is seen that the enzyme activities of animal origin strains (except *L. rhamnosus* BAZ78) are low, while the enzyme activities of human origin strains are higher than other strains.

L. rhamnosus BAZ78 strain with low protein content and high enzyme activity has high specific activity ability, while the strains with high protein content and low enzyme activity (*B. breve* A28 and *B. longum* BASO15) show low specific activity (Table 1). However, although the enzyme activities were high in some strains, a decrease in specific enzyme activities was observed due to the high protein content. To support this situation, Pearson's correlation test was applied and it was seen that there was a moderate negative correlation between protein amount and specific enzyme activity since $r = -0.582$, and this relationship is significant since $p < 0.01$. Since $r = 0.787$ between enzyme activity and protein amount, a high level of positive correlation ($p < 0.01$) was determined. Marazza et al. (2009) reported that they observed the highest specific activity in *L. rhamnosus* CRL981 (22.93 UE/mg) strain in their study and they did not find enzyme activity in the cell supernatant. Tsangalis et al. (2002) reported that Bifidobacterium longum-b strain had β -glucosidase enzyme activity at the amount of 4.625 ± 0.034 U/mg. Choi et al. (2002) determined the β -glucosidase activities of *L. bulgaricus* KCTC 3188, *L. casei* KCTC 3109, *L. delbrueckii* KCTC 1047, *L. delbrueckii* KCTC 1058, and *L. lactis* KCTC 2181 in MRS medium. At the end of the study, the highest β -glucosidase enzyme activity was observed by *L. delbrueckii* subsp. *delbrueckii* KCTC 1047 strain (0.3 units). In addition, it was reported that other strains did not have significant β -glucosidase activity. Yüksekdağ et al. (2018) determined β -glucosidase specific activities of potential probiotic bacteria. The authors reported that β -Glu-specific activity varied from 0.250 to 3.000 U/mg. *L. casei* SC1 (2.750 U/mg), and *L. rhamnosus* EA1 (2.100 U/mg) showed the highest specific activity. In this study, among lactobacilli cultures, the *L. rhamnosus* BAZ78 strain exhibited the best specific activity at 4.500 U/mg and *B. longum* BASO15 (2.330 U/mg) demonstrated the highest specific activity among the bifidobacteria cultures. It was seen that the results obtained from our research were close to other results.

For the β -glucosidase enzyme to be used in industrial applications, it is necessary to determine the most suitable physical conditions in which the enzyme is active, as well as its high enzyme activity. Enzyme reactions are impressed by pH. Amendments in the ionization of prototropic groups in the active centre of the enzyme at low acidic and high alkaline pHs affect the appropriate conformation of the active centre, the binding of the substrate, and the catalysis of the reaction (Koolman & Roehm, 2005). Because pH affects the rate of an enzyme-catalyzed reaction, it is necessary to know its effect on the activity of an enzyme. In this study, the pH of 0.5 M PBS was adjusted to 4.0-8.0 to observe the impact of pH on β -Glu-BAZ78. An increase in enzyme

activity was observed from pH 4.0 to pH 7.5, the highest activity was determined at pH 7.5 (4.500 U/mg) (Table 2), and relative activity was observed to be 52-100% (Figure 1). A decrease in activity was observed after the optimum pH value. In line with all these results, it can be said that the optimum pH value to determine β -glucosidase enzyme activity is 7.5. *L. delbrueckii* subsp. *delbrueckii* KCTC 1047 strain, which showed high β -glucosidase enzyme activity, the optimum pH value was reported as 6.0 (Choi et al. 2002). Marazza et al. (2009) adjusted the pH of 100 mM McIlvaine buffer to 3.0-8.0 to designate the impact of pH on enzyme activity. They determined that the optimum pH value for *L. rhamnosus* CRL981 strain showing high specific activity was 6.4. Sestelo et al. (2004) developed the *Lactobacillus plantarum* strain isolated from wine at pH 4.5-7.5 and determined that the optimum pH value was 5.0. According to the results of the analysis carried out to determine the effect of pH on the specific enzyme activity, it was seen that the optimum pH value differs in all studies. Several amino acids in an enzyme molecule carry a charge. Within the enzyme molecule, positively and negatively charged amino acids will attract (Datta et al., 2017). Changing the pH will impress the ionization state of acidic or basic amino acids. When the pH value of the reaction medium changes, the shape and structure of the enzyme will change. The structure of the enzyme has a strong effect on the enzyme activity and alterations in the structure of the enzyme influence the rate of chemical reactions. It is thought that the differences may be due to these reasons. In addition, differences in the isolation source, buffer, extraction method, and enzyme and substrate concentration of the strains may also be triggers.

Enzyme activity increases with temperature in the temperature range at which enzymes are stable. When the temperature rises above a certain value, a decrease in activity is observed because the enzyme protein will begin to denature (Pamuk, 2011; Kılıç et al., 2014). Therefore, it is significant to determine the temperature value at which the enzyme has high activity and the impact of temperature on enzyme activity.

In the study, the enzyme and specific activities of the β -Glu-BAZ78 were determined at 30° C, 37° C, 40° C, 50° C, and 60° C temperature values. The highest β -glucosidase enzyme and specific activity were observed at 30°C, while the lowest specific activity was detected at 60° C. Relative activity was calculated to be 67-100% (Figure 2). In addition, although specific activity and enzyme activity decreased in the BAZ78 strain at 60° C, an increase in protein amount was observed. This suggests that protein structures can be resistant to high temperatures and this strain could be used commercially. It has been reported that enzyme activity shows effective activity up to 45° C, and enzyme activation decreases above this temperature value (Choi et al., 2002). Marazza et al. (2009) declared that the optimum temperature value for *L. rhamnosus* CRL981 strain was 42° C, while Coulon et al. (1998) reported that *L. casei* ATCC 393 strain had the highest β -glucosidase activity at 35° C. Sestelo et al. (2004) determined the enzyme activity of *L. plantarum* strain at the temperature values of 30-55° C and determined that the enzyme activity was at the highest value at 45° C. Marazza et al. (2009) enzyme at 50° C for 5 min. They found that the β -glucosidase activity of *L. rhamnosus* CRL981 strain decreased by 20% when they were kept waiting, and Sestelo et al.

(2004) found a 50% decrease in the enzyme activity of *L. plantarum* when they applied the same procedure. It is seen that the suitable temperatures for the enzyme activity are different in the studies, and in this study, the enzyme activity changed depending on the temperature.

Determination of the impact of various carbon sources on the growth of microorganisms can provide information about their biotope, particularly the nutrients necessary for their improvement (Alvarez-Zúñiga et al., 2020). In the study, the impact of carbon sources on enzyme activity was determined by growing *L. rhamnosus* BAZ78 strain in different carbon sources (glucose, fructose, sucrose, lactose, cellobiose). It was determined that the BAZ78 strain showed the highest (4.500 U/mg) β -glucosidase-specific enzyme activity in MRS medium containing 2% glucose, and the lowest (1.140 U/mg) in medium containing 2% sucrose. According to the results, relative activity was designated to be 100-152% (Figure 3). Tsangalis et al. (2002) analyzed five strains of Bifidobacteria (*B. pseudolongum*, *B. longum-a*, *B. longum-b*, *B. animalis*, *B. infantis*) in MRS liquid to designate the impact of carbon sources used on enzyme activity. The authors used different carbon resources (MRS-glucose, MRS-lactose, and MRS-raffinose). They declared the specific activity ranges of the strains in their media as follows: 0-0.779 U/mg in MRS, 0-4.625 U/mg in MRS-glucose, 0-3.651 U/mg in MRS-lactose, and 0-0.780 U/mg in MRS-raffinose. Researchers reported that the *B. infantis* strain did not show any enzyme activity in the carbon source used, while other strains had high β -glucosidase activity in MRS-glucose liquid media.

In conclusion, the β -glucosidase enzyme has attracted the attention of both scientists and entrepreneurs due to its industrial importance. Therefore, in this study, it is important to identify probiotic strains with high enzyme activity. For this purpose, *Lactobacillus spp.* (39) and *Bifidobacterium spp.* (3) β -glucosidase enzyme activities, protein amounts, and specific activities of strains were determined. *L. rhamnosus* BAZ78 strain with the highest specific activity among these cultures was used for enzyme optimization studies. To the results obtained, β -Glu-BAZ78 could be used for industrial purposes by being purified.

Acknowledgements

The writers would like to thank Gazi University Academic Writing Application and Research Center (18.5.2022/0076).

Funding Source

This research was supported by Gazi University Scientific Research Projects (BAP) Department (46/2011-01 coded project).

Author Contributions

B.C.A. performed all the experiments and drafted the main manuscript text. B.C.A. and Z.N.Y. designed the experimental work and final versions of the statistics table. Z.N.Y. reviewed and approved the final version of the manuscript.

Conflict of Interest

The authors declare that they have no conflict of interest/competing interests.

References

- Alvarez-Zúñiga, M.T., García, D.C., & Osorio, G. (2020). Effect of different carbon sources on the growth and enzyme production of a toxigenic and a non-toxigenic strain of *Aspergillus flavus*. *Preparative Biochemistry & Biotechnology*, 51(8), 769-779. <https://doi.org/10.1080/10826068.2020.1858426>.
- Ariaeenejad, S., Nooshi-Nedamani, S., Rahban, M., K., Kavousi, Pirbalooti, A.G., Mirghaderi, S.S., Mohammadi, M., Mirzaei, M., & Salekdeh G.H. (2020). A Novel high glucose-tolerant β -Glucosidase: Targeted computational approach for metagenomic screening. *Frontiers in Bioengineering and Biotechnology*, 8, 813, <https://doi.org/10.3389/fbioe.2020.00813>.
- Chen, A., Wang, D., Ji, R., Li, J., Gu, S., Tang, R., & Ji C. (2021). Structural and catalytic characterization of TsBGL, a β -Glucosidase from *Thermofilum sp. ex4484_79*. *Frontiers in Microbiology*, 12, 723678, <https://doi.org/10.3389/fmicb.2021.723678>.
- Choi, Y.B., Kim, K.S., & Rhee, J.S. (2002). Hydrolysis of soybean isoflavone glucosides by lactic acid bacteria. *Biotechnology Letters*, 24, 2113-2116. <https://doi.org/10.1023/A:1021390120400>.
- Coulon, S., Chemarin, P., Gueguen, Y., Arnaud, A., & Galzy P. (1998). Purification and characterization of an intracellular beta-glucosidase from *Lactobacillus casei* ATCC 39. *Applied Biochemistry and Biotechnology*, 74 (2), 105-114. ISSN: 0273-2289.
- Datta, R., Anand, S., Moulick, A., Baraniya, D., Pathan, S.I., Rejsek, K., Vranova, V., Sharma, M., Sharma, D., Kelkar, A., & Formanek P. (2017). How enzymes are adsorbed on soil solid phase and factors limiting its activity: A Review. *International Agrophysics*, 31, 287-302. <https://doi.org/10.1515/intag-2016-0049>.
- Dupont, A., Heinbockel, L., Brandenburg, K., & Hornef M.W. (2014). Antimicrobial peptides and the enteric mucus layer act in concert to protect the intestinal mucosa. *Gut Microbes*, 5(6), 761-765. <https://doi.org/10.4161/19490976.2014.972238>.
- Esteve-Zarzoso, B., Manzaneres, P., Ramon, D., & Querol A. (1998). The role of non-saccharomyces yeasts in industrial winemaking. *International Microbiology*, 1(2), 143-148. <https://doi.org/10.4061/2011/642460>.
- Gao, X., Zhang, M., Li, X., Han, Y., Wu, F., & Liu Y. (2018). The effects of feeding *Lactobacillus pentosus* on growth, immunity, and disease resistance in *Haliotis discus hannai* Ino. *Fish & Shellfish Immunology*. 78, 42-51. <https://doi.org/10.1016/j.fsi.2018.04.010>.

- Garbacz K. (2022). Anticancer activity of lactic acid bacteria. *Seminars in Cancer Biology. Seminars in Cancer Biology*, 83, 3, 356-366. <https://doi.org/10.1016/j.semcancer.2021.12.013>
- Grohmann, K., Manthey, J.A., Cameron, R.G., & Buslig, B.S. (1999). Purification of citrus peel juice and molasses. *Journal of Agricultural and Food Chemistry*, 47(12), 4859-4867. <https://doi.org/10.1021/jf9903049>.
- Huang, R., Zhang, F., Yan, X., Qin, Y., Jiang, J., Liu, Y., & Song, Y. (2021). Characterization of the β -Glucosidase activity in indigenous yeast isolated from wine regions in China. *Journal of Food Science*, 86, 2327-2345. <https://doi.org/10.1111/1750-3841.15741>.
- Kara, H.E., Sinan, S., & Turan, Y. (2011). Purification of beta-glucosidase from olive (*Olea europaea L.*) fruit tissue with specifically designed hydrophobic interaction chromatography and characterization of the purified enzyme. *Journal of Chromatography B*, 879 (19), 1507-1512. <https://doi.org/10.1016/j.jchromb.2011.03.036>.
- Kılıç, Y., Yüksekdağ, Z.N., & Yüksekdağ, H. (2014). Beta-galactosidase enzyme activities of *Lactobacillus* ve *Bifidobacterium* genus. *Journal of Food*, 39(4), 1-8. <https://doi.org/10.5505/gida.29491>.
- Koolman, J., & Roehm, K.H. (2005). *Thieme Color Atlas of Biochemistry*, 2nd Ed Thieme of Stuttgart, 209.
- Kosmerl, E., Rocha-Mendoza, D., Ortega-Anaya, J., Jiménez-Flores, R., & García-Cano, I. (2021). Improving human health with milk fat globule membrane, lactic acid bacteria, and bifidobacteria. *Microorganisms*, 9(2), 341. <https://doi.org/10.3390/microorganisms9020341>.
- Kumar, S., Pattanaik, A.K., Sharma, S. Jadhav, S.E., Dutta, N., & Kumar, A. (2017). Probiotic potential of a *Lactobacillus bacterium* of canine faecal-origin and its impact on select gut health indices and immune response of dogs. *Probiotics Antimicrob Proteins*, <https://doi.org/10.1007/s12602-017-9256-z>.
- Lenz, A.R., Balbinot, E., Oliveira, N.S., Abreu, F.P., Casa, P.L., Camassola, M., Perez-Rueda, E., Silva, S.A., & Dillon, A.J.P. (2022). Analysis of carbohydrate-active enzymes and sugar transporters in *Penicillium echinulatum*: A genome-wide comparative study of the fungal lignocellulolytic system. *Gene*, 822, 146345. <https://doi.org/https://doi.org/10.1016/j.gene.2022.146345>.
- Lu, C., Li, F., Yan, X., Mao, S., & Zhang, T. (2022). Effect of pulsed electric field on soybean isoflavone glycosides hydrolysis by β -glucosidase: Investigation on enzyme characteristics

and assisted reaction. *Food Chemistry*, 378, 132032.
<https://doi.org/https://doi.org/10.1016/j.foodchem.2021.132032>.

Maldonado, J., Gil-Campos, M., Maldonado-Lobón, J.A., Benavides, M.R., Flores-Rojas, K., Jaldo, R., Jiménez del Barco, I., Bolívar, V., Valero, A.D., Prados, E., Peñalver, I., & Olivares, M. (2019). Evaluation of the safety, tolerance and efficacy of 1-year consumption of infant formula supplemented with *Lactobacillus fermentum* CECT5716 Lc40 or *Bifidobacterium breve* CECT7263: A randomized controlled trial. *BMC Pediatric*, 19, 361.
<https://doi.org/10.1186/s12887-019-1753-7>.

Marazza, J.A., Garro, M.S., & Giori, G.S. (2009). Aglycone production by *Lactobacillus rhamnosus* CRL981 during soymilk fermentation. *Food Microbiology*, 26, 333-339.
<https://doi.org/10.1016/j.fm.2008.11.004>.

Meng, F., Yang, S., Wang, X., Chen, T., Wang, X., Tang, X., Zhang, R., & Shen, L. (2017). Reclamation of Chinese herb residues using probiotics and evaluation of their beneficial effect on pathogen infection. *Journal of Infection and Public Health*, 10(6), 749-754.
<https://doi.org/http://dx.doi.org/10.1016/j.jiph.2016.11.013>.

Modrackova, N., Vlkova, E., Tejnecky, V., Schwab, C., & Neuzil-Bunesova, V. (2020). Bifidobacterium β -Glucosidase activity and fermentation of dietary plant glucosides are species and strain-specific. *Microorganisms*, 8, 839.
<https://doi.org/10.3390/microorganisms8060839>.

Naidu, A.S., Bidlack, W.R., & Clemens, R.A. (1999). Probiotic spectra of lactic acid bacteria (LAB). *Critical Reviews in Food Science and Nutrition*, 39:1, 13-126.
<https://doi.org/10.1080/10408699991279187>.

O'Callaghan, A., & van Sinderen D. (2016). Bifidobacteria and their role as members of the human gut microbiota. *Frontiers in Microbiology*, <https://doi.org/10.3389/fmicb.2016.00925>.

Pamuk, F. (2011). *Biyokimya*. Gazi Kitabevi, Ankara, Türkiye, 272s.

Pang, P., Cao, L-c., Liu, Y-h., Xie, W., & Wang, Z. (2017). Structures of a glucose-tolerant β -glucosidase provide insights into its mechanism. *Journal of Structural Biology*, 198(3), 154-162. <http://dx.doi.org/10.1016/j.jsb.2017.02.001>.






Seidel, Z.P., & Lee, T. (2020). Enhanced activity of the cellulase enzyme β -Glucosidase upon addition of an azobenzene-based surfactant. *ACS Sustainable Chemistry and Engineering*, 8, 4, 1751-1761. <https://doi.org/10.1021/acssuschemeng.9b05240>.

- Sener, A. (2015). Extraction, partial purification and determination of some biochemical properties of β -glucosidase from Tea Leaves (*Camellia sinensis* L.). *Journal of Food Science and Technology*, 52(12), 8322-8328. <https://doi.org/10.1007/s13197-015-1915-z>.
- Sestelo, A.B.F., Poza, M., Viilla T.G. (2004). β -Glucosidase activity in a *Lactobacillus plantarum* wine strain. *World Journal of Microbiology & Biotechnology*, 20, 633-637.
- Singh, G., Verma, A.K., & Kumar, V. (2016). Catalytic properties, functional attributes and industrial applications of β -glucosidases. *Biotechnology*, 6:3. <https://doi.org/10.1007/s13205-015-0328-z>.
- Singhania, R.R., Patel, A.K., Sukumaran, R.K., Larroche, C., & Pandey, A. (2013). Role and significance of beta-glucosidases in the hydrolysis of cellulose for bioethanol production. *Bioresour Technology*. 127(1), 500-7. <https://doi.org/10.1016/j.biortech.2012.09.012>.
- Strahsburger, E., Lacey, M.L.L., Marotti, I., DiGioia, D., Biavati, B., & Dinelli, G. (2017). In vivo assay to identify bacteria with β -glucosidase activity. *Electronic Journal of Biotechnology*, 30, 83-87. <https://doi.org/10.1016/j.ejbt.2017.08.010>.
- Tamaki, F.K., Souza, D.P., Souza, V.P., Ikegami, C.M., Farah, C.S., & Marana, S.R. (2016). Using the amino acid network to modulate the hydrolytic activity of β -Glycosidases. *PLoS One*, 11(12). <http://doi.org/10.1371/journal.pone.0167978>.
- Temizkan, G., Yılmaz, S., Öztürk, M., Arı, Ş., Ertan, H., Sarıkaya, A.T., & Arda, N. (2008). *Moleküler Biyolojide Kullanılan Yöntemler*. İstanbul Üniversitesi Biyoteknoloji ve Genetik Mühendisliği Araştırma ve Uygulama Merkezi (Biyogem) Yayın, Nobel Tıp Kitapevleri, 345s.
- Teugjas, H., & Våljamäe, P. (2013). Selecting β -glucosidases to support cellulases in cellulose saccharification. *Biotechnology for Biofuels and Bioproducts*, 6, 105. <https://doi.org/http://www.biotechnologyforbiofuels.com/content/6/1/105>.
- Tsangalis, D., Ashton, J.F., McGill, A.E.J., & Shah, N.P. (2002). Enzymic transformation of isoflavone phytoestrogens in soymilk by β -glucosidase producing bifidobacteria. *Journal of Food Science*, 67, 8, 3104-3113. <https://doi.org/10.1111/j.1365-2621.2002.tb08866.x>.
- Yüksekdağ, Z., Cinar Acar, B., Aslim, B., & Tukenmez, U. (2018). β -Glucosidase activity and bioconversion of isoflavone glycosides to aglycones by potential probiotic bacteria. *International Journal of Food Properties*, 20, S3. S2878-2886. <https://doi.org/10.1080/10942912.2017.1382506>.

- Yüksekdağ, H., & Yüksekdağ, Z. (2021). Beta-galactosidase activity in *Lactobacillus delbrueckii* subsp. *bulgaricus* ZN541 and *Streptococcus thermophilus* Z1052 strains and optimization. *The Journal of Food*, 46(6), 1331-1342. <https://doi.org/10.15237/gida.GD21059>.
- Zang, X., Liu, M., Fan, Y., Xu, J., Xu, X., & Li, H. (2018). The structural and functional contributions of β -glucosidase-producing microbial communities to cellulose degradation in composting. *Biotechnology Biofuels*, 11:51. <https://doi.org/10.1186/s13068-018-1045-8>.
- Zhu, L., Mu, T., Ma, M., Sun, H., & Zhao, G. (2022). Nutritional composition, antioxidant activity, volatile compounds, and stability properties of sweet potato residues fermented with selected lactic acid bacteria and bifidobacteria. *Food Chemistry*, 374, 131500. <https://doi.org/10.1016/j.foodchem.2021.131500>.



BUSER Transcutaneous Electric Nerve Stimulator Device Design

Gökhan Nur ^{1*} , Büşra Nur Barış ¹ , Büşra Levent ¹ , Buse Selin Sazaklıoğlu ¹ ,
Elvan Ak ² 

¹ Department of Biomedical Engineering, Faculty of Engineering and Natural Sciences, Iskenderun Technical University, Hatay, Türkiye.

² Ministry of Health, Hatay Provincial Health Directorate, Healthy Nutrition and Active Life Unit, Hatay, Türkiye.

Abstract

The Transcutaneous Electrical Nerve Stimulator (TENS) is one of the medical devices that uses electricity to stimulate the nerve and produce analgesic effects. A TENS device is a small battery-powered or city-powered device with ends attached to sticky pads called electrodes. TENS, with its main purpose of helping to reduce pain and muscle spasms, has a wide usage area, especially in arthritis, fibromyalgia, chronic pelvic pain, knee pain, menstrual pain, low back pain, sports injuries, and atrophic muscle tissue cases. In this study, a Transcutaneous electrical stimulation device, which is one of the physical therapy methods performed by applying electrical energy, was designed. Designed device; it is easy to use, low cost, and suitable for patients, and arduino is used for integration and programming.

Keywords:

TENS device, gate-control theory, oscilloscope, pertinax, breadboard

Article history:

Received 10 December 2022, Accepted 15 February 2023, Available online 10 April 2023

Introduction

Transcutaneous electrical nerve stimulation (TENS) is a non-invasive, safe, easy-to-apply, portable, and inexpensive technique that provides pulsed electrical stimulation that can be varied in frequency, current intensity, and duration. The concept of TENS has historically been the subject of heated debate in scientific circles in terms of effectiveness. However, although this method of

*Corresponding Author: Gökhan NUR, E-mail: gokhan.nur@iste.edu.tr

pain management has proven itself in clinical trials, there is disagreement to date about which pain syndromes and conditions TENS is appropriate for (Teoli & Ann, 2022). It has the advantage of allowing patients to control their pain autonomously through two or more skin electrodes to stimulate subcutaneous nerves for pain control (Pal et al., 2020). As a non-invasive analgesic therapy, transcutaneous electrical nerve stimulation is widely used to relieve pain in various clinical applications by delivering current pulses to the skin area to activate peripheral nerve fibers (Mokhtari et al., 2020). In the TENS device, the pads are attached directly to the skin. When the machine is turned on, small electrical pulses are delivered to the affected area of the body, which is felt as a tingling sensation. Electrical impulses can reduce pain signals to the spinal cord and brain, which can help relieve pain and relax muscles. These signals are first transmitted to the nerves located under the skin and from there to the brain via nerves. The sense of pain reaching the brain itself is replaced by electrical currents and thus the pain becomes undetectable. In fact, the pains continue in the body and the pain harms the body. The TENS device is only a method that prevents the perception of this pain to the brain. They can also stimulate the production of endorphins, which are the body's natural pain relievers (Johnson & Jones, 2017). TENS is used clinically by various healthcare professionals for the reduction of pain. The clinical effectiveness of TENS is controversial, with some studies supporting it while others rejecting its clinical use (Sluka & Walsh, 2003). Compared to many drugs, the device does not pose a risk of overdose. TENS units are generally highly adjustable, allowing the user to control pulse width, intensity and frequency. The low frequency of < 10 Hz in conjunction with the high intensity is used to generate muscle contractions. High frequencies > 50 Hz are used at low intensity to induce paresthesia without muscle contractions (Teoli & Ann, 2022).

This study, it is aimed to design the Transcutaneous electrical stimulation (TENS) device, which is the most useful form of electrotherapy technique commonly used in physical therapy methods, with a 2-mode and single-channel output system, unlike the ones on the market, and which applies low-voltage electric current.

Materials and Methods

Circuit Information

The circuit diagram shown in Figure 1 was taken as a reference and the materials were selected and the circuit diagram was drawn with the Proteus 8.1 Professional program. It was transferred to Ares 8.1 Professional environment after open circuit drawing. As indicated in Figure 2, the lines drawn between the circuit elements were selected in the T60-T80 range, the lines were placed more prominently in the printed circuit and they were designed in such a way that they would not come into contact with each other by adding a terminal block. In order to create the printed circuit, the drawings were transferred to Ares via Proteus and the paths in the printed circuit were made ready.

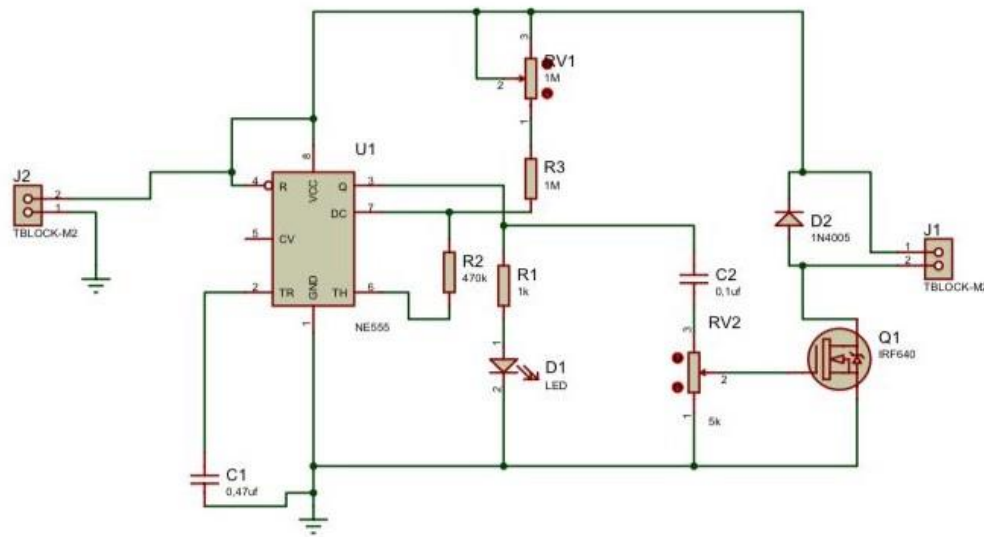


Figure 1. Open circuit diagram of the transcutaneous electrical stimulation (TENS) device

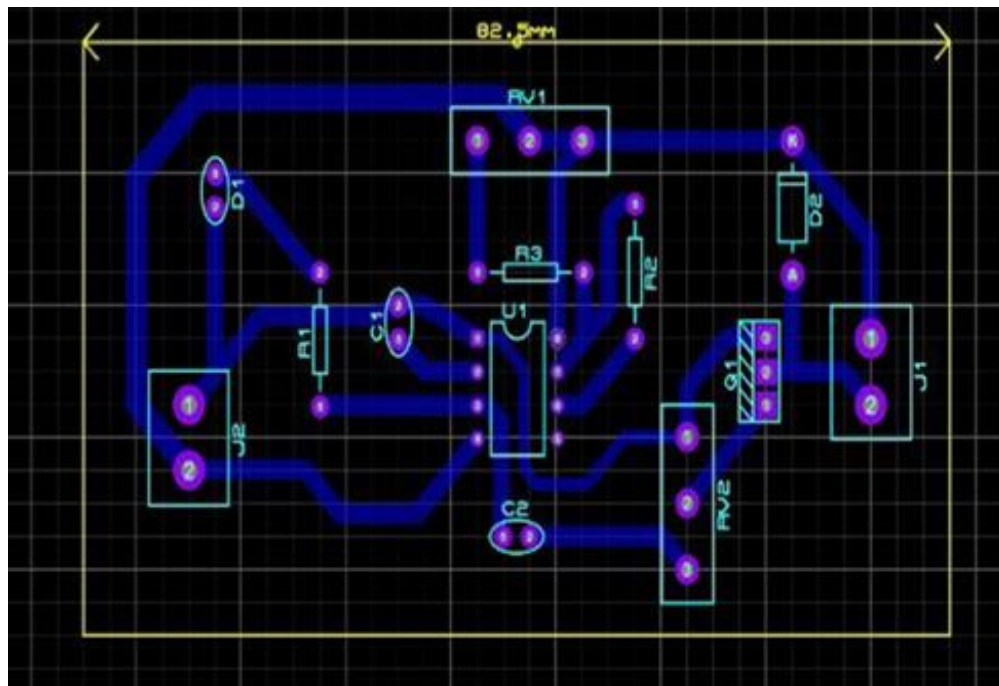


Figure 2. Printed circuit drawing

Print Circuit Stages

The printed circuit drawing in Figure 2 was printed on transfer paper by trying several dimensions. Printed using a laser printer as printer to transfer the toner with heat. Before the heat treatment, the

plate was sanded and cleaned, and it was aimed to transfer the toner onto the pertinax without any problems. In order to transfer the circuit diagram on the transfer paper to the pertinax, the surface of the print was transferred to the plate by contacting the surface with heat for an average of 5 minutes, as shown in Figure 3. This step should be followed carefully and the iron should be moved to different points of the paper and at different angles, as deterioration may occur in the paths that are tried to be transferred in case of excessive heat exposure.



Figure 3. Passing the circuit to the pertinax with the help of heat

When the transfer paper heats up, the toner is transferred onto the plate. After this stage, the paper and pertinax are exposed to water in Figure 4 in order not to damage the roads, so that the sticking parts get wet and the transfer paper is removed more easily and without damaging the roads. By cleaning the circuit with the help of sandpaper, scratches were obtained on the copper.



Figure 4. Separation of transfer paper over pertinax



Figure 5. Melting of copper plate in solution

In the continuation of this application, the pertinax plate with the circuit lines removed is thrown into the solution prepared with 1/3 salt spirit and Hydrogen Peroxide in the mixing bowl in Figure 5, and it melts the copper in an average of 15 seconds, causing color change and steam output in the liquid. In order not to inhale the steam, it should be carried out in the open area or by wearing a mask, skin and clothing contact should be avoided. At the end of 15 seconds, the paths on the pertinax become clear. However, one of the points to be considered is that in case some of

the roads do not come out completely, they should be thrown back into the solution and the lines should be clarified by careful follow-up. If it is kept in the solution for too long, the copper plate may melt. For this reason, when the plaque was removed from the solution, it was immediately purged from water or pertinax solution by means of a solution and after making sure that it was thoroughly dried, 35 holes were drilled with a 1.0 mm drill bit to place the circuit elements on the pertinax (Figure 6, Figure 7).



Figure 6. Opening the slots of the components that will be mounted on the circuit

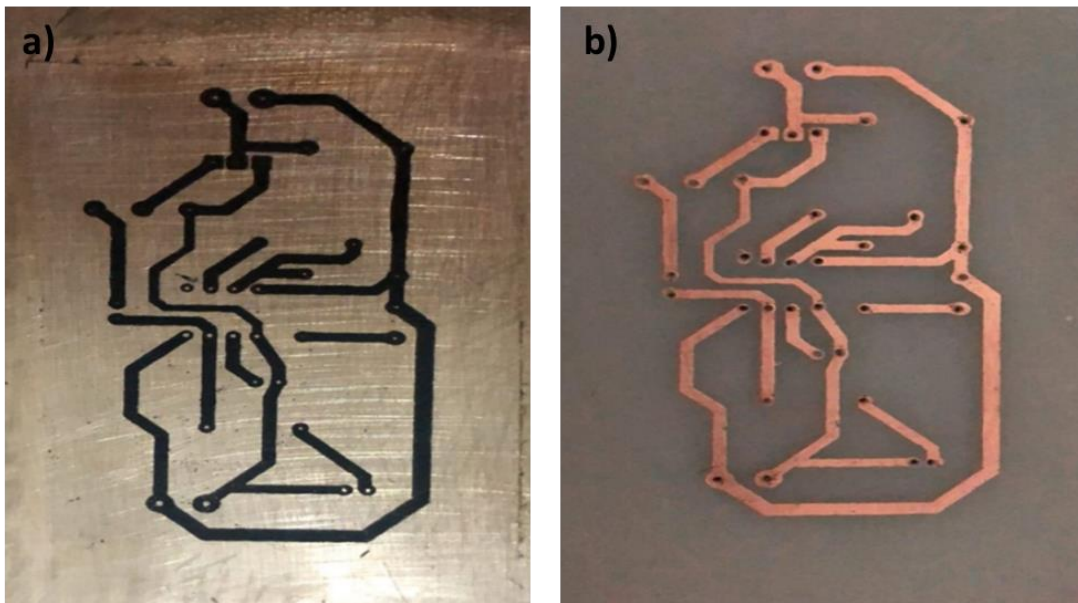


Figure 7. a) The version before Pertinax was thrown into solution. b) A drilled version of the slots after Pertinax is thrown into the solution

After the printing circuit phase was completed, the elements in the circuit were placed on the breadboard and tested with the buzzer mode of the multimeter. As seen in Figure 8, when the red led is on, it is an indication that the circuit is in working condition.

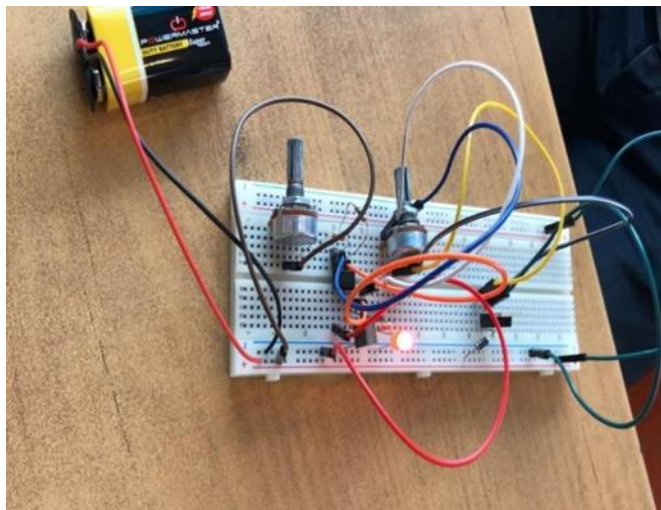


Figure 8. Running the circuit on the breadboard

Circuit elements were placed in the slots opened on the pertinax in the post-stage of the circuit, which was prepared and running smoothly, as indicated in Figure 7, and soldered, and the long legs were cut off as seen in Figure 9.

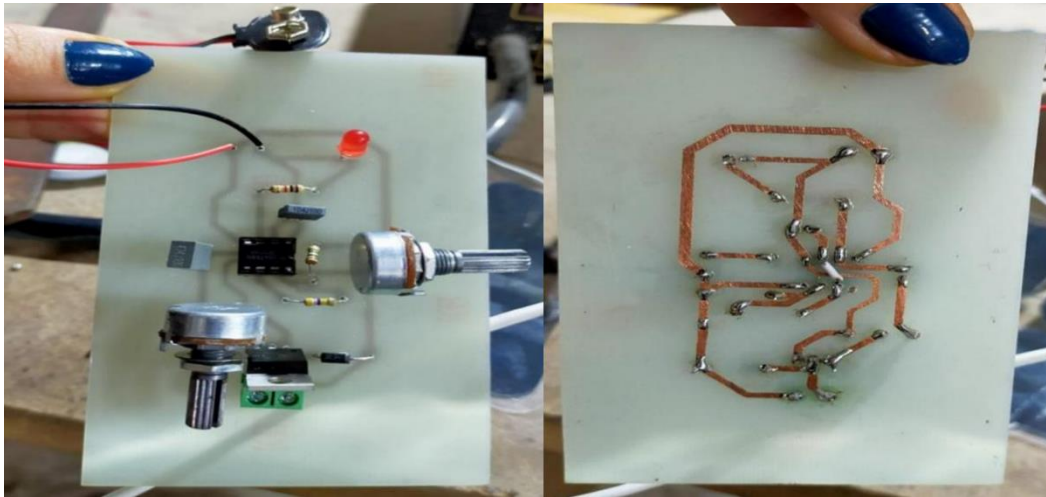


Figure 9. Front view and soldered rear view of the circuit elements on the pertinax

Results

There are two types of users in the designed system. In one use, it is possible to be isolated from the mains and used a mobile with a dry battery. For other uses that require higher current, it is possible to use it by means. While establishing the circuit, the N555, which is inexpensive and easy to access, is used. 1 M pot was used to adjust the frequency of the circuit. The frequency of the circuit is adjusted in the range of 1-100 Hz with the help of a potentiometer. The frequency range can be further increased thanks to the potentiometer. In addition, it has been established in such a way that the amplitude of the output voltage can be adjusted with a potentiometer. The frequency range is adjusted by triggering the N555 with a 1 M resistor and 470 K resistors. The trigger voltage of the 5 K pot IRF640 MOSFET is regulated and the amplitude of the output wave is adjusted. The IRF640 also acts as a switch that triggers the transformer. 0.47 μF capacitor is connected to the reset pin to trigger N555. A 0.1 μF capacitor has been added to the circuit to prevent interference with the MOSFET. On the other hand, the 1N4005 diode is used to prevent reverse currents from the transformer. The reason for integrating the transformer into the circuit is that the transformer provides isolation from the body and brings the voltage to the appropriate level. The red led used here is used as an indicator showing the range of signal pulses coming to the probes and it flashes simultaneously with the pulse frequency. In order to prevent the LED from burning, a 1K resistor is added to the circuit. Another purpose of the LED is to act as a stimulus used to show whether the circuit is working or not. The probes added to the circuit transmit signals to the body by providing the connection between the body and the circuit. The task of the two probes available is to complete the circuit. Because one probe acts as a receiver and the other probe act as a transmitter. The human body acts as a transmitter between the two probes.

The BUSER brand TENS device designed in the study was compared with the Fizyopol brand TENS device sold in the market. There are three different programs in the Fizyopol brand

TENS device. These; include TENS mode, EMS mode, and Massage mode. These programs are divided into modes within themselves. There are 9 programs in the TENS mode. Among the reasons for leaving the programs; Sensitivity (pain threshold), which can vary according to the person, the severity of the pain, the location, and the change in the frequency of recurrence can be counted. There are 8 programs in EMS mode and 5 programs in the Massage program. The device has a total of two channels, four electrode outputs, and a pack of 5x5 TENS pads. The frequency of this device is in the range of 1-100 Hz and the output power is 0.120 mA. The designed BUSER TENS device can be used in two modes, and in these uses, the ampere intensity of the device changes according to the type of treatment. The device includes a single channel and 2 electrode outputs. Its frequency is in the range of 1-100 Hz.

In order to observe the time-dependent changes in the electrical voltage between the designed system and the Fizyopol brand TENS device, the differences of the system with standard TENS devices were determined by comparing the current waves on the two-axis graph on the oscilloscope screen. The wavelengths of the Fizyopol brand TENS device connected to the CH1 port of the oscilloscope are shown in yellow in Figure 10. Shown in blue are the wavelengths of the BUSER TENS device connected to the CH2 port. The sine waves produced when the devices send regular current are shown in Figure 10. While the Fizyopol brand sends high currents at regular intervals, BUSER continues to send regular currents. This difference is shown in Figure 10.



Figure 10. a) Regularly generated sine waves of Fizyopol brand TENS and BUSER TENS. b) Oscilloscope image when Fizyopol TENS device and BUSER TENS device pulse

Discussion

Transcutaneous electrical nerve stimulation (TENS) is a physical therapy method commonly used in the treatment of pain (Vance et al., 2012; Santuzzi et al., 2013). It is used as a technique with successful results in the reduction of fibromyalgia (Dailey et al., 2022), primary dysmenorrhea pain (Arik et al., 2022), shoulder pain (Bilek et al., 2021), back pain (Vella et al., 2022) and chronic cancer pain (Katta et al., 2022). TENS enhances local inhibitory control and is indicated in focal

neuropathic pain (NP) (Guastella et al., 2008). The analgesic effect of TENS is similar to that obtained with opioid agonists in the treatment of NP (Kim et al., 2003). TENS is a noninvasive method that is easy to apply with relatively few contraindications.

When Doğan & Kılınçdemir (2017) examined, they aimed to have a low cost, unlike standard and market modules. For this, they designed the TENS device as an analog and used a very inexpensive small circuit working with a 9 V battery in their project. They added the PIC16F877A to the device, which was designed according to the household TENS device and converted from manual use to digital use. In the future planning of their projects, they stated that they could develop the TENS device more professionally by giving an electrical signal that takes the opposite of the pain signal and applies it to the body (Doğan & Kılınçdemir, 2017). In addition to this study, the difference and innovation of the device designed in Buran's study are; It is the automatic application of TENS modalities used in different pain patterns, acting through different mechanisms, to the patient as a program with the help of a microcontroller (Buran, 2002). In the TENS device designed by Uysal to apply to acupuncture points, arduino has been used for options, integrations, and programming that can be changed for treatment programs suitable for the use of patients. Device; It offers three different options frequency, current strength, and pulse width adjustment (Uysal, 2018). In Güzel's work, she designed the EMS (electrical muscle stimulation) device, which has a TENS-like function. This device has electromagnetic compatibility (SAR) with the human body, which is around 1% of the maximum values (Güzel, 2018). In a study, it was stated that the TENS device significantly reduced pain and improved walking ability in people with knee osteoarthritis (KO) (Wu et al., 2022). Most of the studies have been carried out to confirm that the electrical properties of TENS are consistent with the properties provided by a standard TENS device (Johnson et al., 2022). As we have observed as a result of our literature research, not many innovations have been made on TENS on their own, but steps have been taken to improve it. There are many TENS devices with different features and they apply different wavelength signals according to the type of pain. In this way, pain is relieved without exposing the body to any medication and without side effects. Today, the use of TENS devices has become quite common thanks to this and similar ease of use.

In conclusion, the difference between this designed device from the ones on the market and other works is that it offers the opportunity to be connected to the city network with a system that provides single-channel output with 2 modes for ease of use, as well as the opportunity to be used as a home type with a 9 Volt battery. Thus, the space limit for access to treatment has been eliminated. The device becomes active by opening the power button that starts the electric current. Then, by increasing the current adjusting button, it is ensured that the user reaches the current form that will relieve the discomfort and relax the user. It is possible to make the device more portable by reducing the transformer where the output power is supplied. Modules can be added by adding PIC or other functional programs in the future by making research and observations for the

development of the design. A more functional appearance and service can be achieved by developing a dynamic design suitable for the network-connected and home-use versions.

Acknowledgements

This study was presented orally at the 4th International Conference on Applied Engineering and Natural Sciences (November 10-13, ICAENS-2022).

Author Contributions

Dr. Nur, MSc. Ak, MSc. Levent, MSc. Barış and MSc. Sazaklıoğlu researched the literature and designed the study. They were interested in protocol development, and experimental design. All authors reviewed and edited the article and approved the final version of the article.

Conflict of Interest

The authors declared that no conflict of interest.

References

- Arik, M. I., Kiloatar, H., Aslan, B., & Icelli, M. (2022). The effect of TENS for pain relief in women with primary dysmenorrhea: A systematic review and meta-analysis. *Explore-The Journal of Science and Healing* 18(1), 108-113. <https://doi.org/10.1016/j.explore.2020.08.005>.
- Bilek, F., Karakaya, M. G., & Karakaya, İ. Ç. (2021). Immediate effects of TENS and HVPS on pain and range of motion in subacromial pain syndrome: A randomized, placebo-controlled, crossover trial. *Journal of Back and Musculoskeletal Rehabilitation*, 34(5), 805-811. <https://doi.org/10.3233/BMR-191833>.
- Buran, R. (2002). Fizik tedavi yöntemleri ve mikrodenetleyici ile tens tasarımı. İstanbul Teknik Üniversitesi, Fen Bilimleri Enstitüsü, Elektronik ve Haberleşme Mühendisliği Anabilim Dalı, Yüksek Lisans Tezi, İstanbul.
- Dailey, D. L., Vance, C. G. T., Chimenti, R., Rakel, B. A., Zimmerman, M. B., Williams, J. M., Sluka, K. A., & Crofford, L. J. (2022). The Influence of Opioids on Transcutaneous Electrical Nerve Stimulation Effects in Women With Fibromyalgia. *The Journal of Pain*, 23(7), 1268-1281. <https://doi.org/10.1016/j.jpain.2022.02.008>.
- Doğan, O., & Kılınçdemir, M. (2017). Tens cihazı. Yakın Doğu Üniversitesi, Biyomedikal Mühendisliği Bölümü, Bitirme Projesi, Lefkoşa.
- Guastella, V., Mick, G., & Laurent, B. (2008). Non-pharmacologic treatment of neuropathic pain. *Presse Medicale*, 37(2 Pt 2), 354-7. <https://doi.org/10.1016/j.lpm.2007.11.008>.

- Güzel Ş. (2018). Ergonomik EMS (elektro kas uyarım) Sistemi ile Diyabetik Polinöropati Ağrı Etkilerinin Azaltılması. Erciyes Üniversitesi, Fen Bilimleri Enstitüsü, Mekatronik Mühendisliği Anabilim Dalı, Yüksek Lisans Tezi, Kayseri.
- Johnson, M. I., & Jones, G. (2017). Transcutaneous electrical nerve stimulation: current status of evidence. *Pain Management*, 7(1), 1-4. <https://doi.org/10.2217/pmt-2016-0030>.
- Johnson, M. I., Paley, C. A., Wittkopf, P. G., Mulvey, M. R., & Jones, G. (2022). Characterising the Features of 381 Clinical Studies Evaluating Transcutaneous Electrical Nerve Stimulation (TENS) for Pain Relief: A Secondary Analysis of the Meta-TENS Study to Improve Future Research. *Medicina*, 58(6), 803. <https://doi.org/10.3390/medicina58060803>.
- Katta, M.R., Valisekka, S. S., Agarwal, P., Hameed, M., Shivam, S., Kaur, J., Prasad, S., Bethineedi, L. D., Lavu, D. V., & Katamreddy, Y. (2022). Non-pharmacological integrative therapies for chronic cancer pain. *Journal of Oncology Pharmacy Practice*, 9:10781552221098437. <https://doi.org/10.1177/10781552221098437>.
- Kim, J., Jung, J. I., Na, H. S., Hong, S. K., & Yoon, Y. W. (2003). Effects of morphine on mechanical allodynia in a rat model of central neuropathic pain. *Neuroreport*, 14(7), 1017-20. <https://doi.org/10.1097/01.wnr.0000070190.28954.ec>.
- Mokhtari, T., Ren, Q., Li, N., Wang, F., Bi, Y., & Hu, L. (2020). Transcutaneous Electrical Nerve Stimulation in Relieving Neuropathic Pain: Basic Mechanisms and Clinical Applications. *Current Pain and Headache Reports*, 24(4):14. <https://doi.org/10.1007/s11916-020-0846-1>.
- Pal, S., Dixit, R., Moe, S., Godinho, M. A., Abas, A. B., Ballas, S. K., Ram, S., & Yousuf, U. A. M. (2020). Transcutaneous electrical nerve stimulation (TENS) for pain management in sickle cell disease. *Cochrane Database of Systematic Reviews*, 3(3):CD012762. <https://doi.org/10.1002/14651858.CD012762.pub2>.
- Santuzzi, C. H., Neto Hde, A., Pires, J. G., Gonçalves, W. L., Gouvea, S. A., & Abreu, G. R. (2013). High-frequency transcutaneous electrical nerve stimulation reduces pain and cardio-respiratory parameters in an animal model of acute pain: Participation of peripheral serotonin. *Physiotherapy Theory and Practice*, 29(8), 630-8. <https://doi.org/10.3109/09593985.2013.774451>.
- Sluka, K. A., & Walsh, D. (2003). Transcutaneous electrical nerve stimulation: Basic science mechanisms and clinical effectiveness. *The Journal of Pain*, 4(3), 109-21. <https://doi.org/10.1054/jpai.2003.434>.

- Teoli, D., & An, J. (2022). Transcutaneous Electrical Nerve Stimulation. [Updated 2022 May 26]. In: StatPearls [Internet]. Treasure Island (FL): StatPearls Publishing; 2022 Jan-. Available from: <https://www.ncbi.nlm.nih.gov/books/NBK537188/>.
- Uysal, R. (2018). Tens Device Design for Stimulation of the Acupuncture Points. Near East University, Graduate Scholl of Applied Sciences, Department of Biomedical Engineering, Master Thesis, Nicosia.
- Vance, C. G., Rakel, B. A., Blodgett, N. P., DeSantana, J. M., Amendola, A., Zimmerman, M. B., Walsh, D. M., & Sluka, K. A. (2012). Effects of transcutaneous electrical nerve stimulation on pain, pain sensitivity, and function in people with knee osteoarthritis: a randomized controlled trial. *Physical Therapy*, 92(7), 898-910. <https://doi.org/10.2522/ptj.20110183>.
- Vella, S. P., Chen, Q., Maher, C. G., Simpson, P. M., Swain, M. S., & Machado, G. C. (2022). Paramedic management of back pain: a scoping review. *BMC Emergency Medicine*, 22(1), 144. <https://doi.org/10.1186/s12873-022-00699-1>.
- Wu, Y., Zhu, F., Chen, W., & Zhang, M. (2022). Effects of transcutaneous electrical nerve stimulation (TENS) in people with knee osteoarthritis: A systematic review and meta-analysis. *Clinical Rehabilitation*, 36(4), 472-485. <https://doi.org/10.1177/02692155211065636>.



Parameters Response of Salt-Silicon Interactions in Wheat

Mehmet Hanifi Akgün , Nuray Ergün * 

Hatay Mustafa Kemal University, Science and Art Faculty, Biology Department,
Hatay, Türkiye.

Abstract

Wheat is the most important plant in the history of mankind, especially in terms of nutrition, by increasing its resistance from the past to the present. The negative change in the environmental conditions increases the stress factors in the soil and seriously affects agricultural productivity. Some physiological analyzes were carried out to examine salt, silicon and salt-silicon interactions on wheat seedlings. In the present study salt, silicon, salt–silicon and their interactions were investigated on wheat (*Triticum aestivum* L cv. Dağdaş and ES-14). Root dry weight, shoot dry weight, shoot and root length. In our study; Si increased shoot dry matter and weight in 200 mM salt+ Si treatment.

Keywords:

Root dry weight, shoot dry weight, shoot length, root length.

Article history:

Received 5 September 2022, Accepted 17 December 2022, Available online 10 April 2023

Introduction

Abiotic stress factors such as salinity, drought and chills cause significant loss of yield in terms of plant growth and development. It is becoming more important to reduce this loss of yield in agricultural products and to shed light on these mechanisms & osmotic stress caused by salt stress, compete with ions such as K^+ and Ca^{2+} , which are necessary for the plant, and reduce the uptake of these elements (Hu & Schmidhalter, 2005; Guo et al., 2021). NaCl stress makes negative effects on the chloroplast organelle. It causes ROS accumulation by resulting in swelling in stroma and thylakoids (Çulha & Çakırlar, 2011). It was reported that NaCl stress reduced dry and wet weight in the stem, reduced chlorophyll content (Rohanipoor et al., 2013) as well as seed in fruit, dry matter amount and seed weight (Kardoni et al., 2013; Farooq et al., 2019). Also, Kahrizi et al. (2012) reported that antioxidant enzymes changed POX, SOD, CAT and ATPase activity. Also, it

*Corresponding Author: Nuray ERGÜN, E-mail: ergun.nuray@gmail.com

was reported that the proportional water amount decreased, free proline amount increased (Öncel & Keleş, 2002), water intake decreased and germination decreased (Rahman et al., 2008).

Silicon contributes to the growth of wheat under salt stress by inhibiting Na uptake, providing nutritional balance and improving physiological parameters (Javaid et al., 2019). Although Silicon (Si) is the second most abundant element on earth, it is not yet included in the list of essential elements for plants. However, the useful effect of Si on growth and development in many plant varieties is striking. In soil, Si is generally available in the form of silicic acid (H_4SiO_4), and the uptake of Si by plants differs among plant families. The Poaceae generally take Si much more than the other species (Reichert et al., 2015). It is known that Si reduces the harmful effects of heavy metal stress such as Si, manganese, aluminium, salt, drought, chill and freezing stresses (Liang et al., 2006). However, there is not sufficient information on the role of Si in abiotic stresses.

In this study, mean root and shoot dry weights, root and shoot lengths, were analyzed in wheat (*Triticum aestivum* L. cv. Dağdaş and ES-14) seedlings in NaCl, Si and NaCl+ Si interactions.

Materials and Methods

Seeds (*Triticum aestivum* L. cv. Dağdaş, ES-14) were used as plant material. The wheat seeds were obtained from Field Crops Central Research Institute (Ankara). In the process of growing the wheat, seeds were sterilized with a solution including 2% sodium hypochlorite (NaOCl) (Rubio et al., 1994) for 20 minutes and then washed with distilled water. The seeds were grown in wooden containers containing perlite and watered with distilled water for five days in the climate cabin. Arnon and Hoagland's solution (Arnon & Hoagland, 1940) adjusted to pH 5.7 was used as a nutrient solution. On the 5th day, the solutions in the containers were discharged, and they were filled with new nutrient solutions. When the seedlings were 15 days old were performed by mixing Salt and Si treatments them into the nutrient solutions. After the sixth day, four different groups were formed, which are as follows: NaCl 150 mM, NaCl 200 mM, NaCl 150 mM+Si 1 mM, NaCl 200 mM+Si 1 mM and Si 1 mM. The roots of the seedlings spared for biochemical analysis were cut from the root-shoot separation zone.

Results

In Dağdaş cultivar, 200 mM NaCl treatment decreased root length while 150 mM NaCl+1 mM Si and 200 mM NaCl+1 mM Si treatments led to increases when compared to the control group (Table 1).

Table 1. Effects of NaCl and NaCl -Si interactions on average root and shoot length, root and shoot dry weight of wheat (*Triticum aestivum* L.cv.) Dağdaş and ES-14 seedlings (cm/plant) (n = 3).

	Root length (cm/plant)		Root dry weight (mg/plant)	
	Dağdaş	ES-14	Dağdaş	ES-14
CONTROL	9.7± 0.416	9.633±0.669	4.666±0,333	3.266±0.266
1mM Si	9.573± 0.436	10.866±0.328	1±0	6±0.577
150 mM NaCl	10.5± 0.871	8.166±0.811	4.2±0,20	2±0
150 mM NaCl +1mM Si	11.306±0.619	8.7±0.360	5±0,577	3±0
200 mM NaCl	8.293± 0.522	9.053±0.177	2±0	4±0
200 Mm NaCl+1mMSi	10.433±1.04	8.5±0.288	2.233±0,333	5.333±0.333
	Shoot length (cm/plant)		Shoot dry weight (mg/plant)	
	Dağdaş	ES-14	Dağdaş	ES-14
CONTROL	23.4± 0.750	18.5± 2.203	15.733±0,896	15.933±1.572
1mM Si	22.1± 0.556	17.566± 0.433	16.333±0,881	13.666±0.666
150 mM NaCl	22.926±1.268	15.8± 0.781	14.133±0,696	13±1
150 mM NaCl +1mM Si	23.733±0.433	17.833± 0.371	15.466±0,29	15.2±0.416
200 mM NaCl	20.4± 0.503	16.266± 0.233	11.666±0,881	14.333±1.201
200mM NaCl +1 mM Si	22.766± 0.29	16.566± 0.317	18±1	15.333±0.666

These results are in line with those obtained by Rohanipoor et al. (2013) in corn plants under NaCl stress. According to Table 1, there is an increase in the ES-14 cultivar compared to the control group in 1 mM Si treatment. Also, decreases obtained in the treatments containing NaCl are consistent with the data reported by Rohanipoor et al. (2013) with corn plants under salt stress. It is known that NaCl stress reduces the uptake of elements such as K, which are essential for plants (Ali et al., 2012). Elements such as K play a key role in the development of plant growth. In all treatments where salt was added in the ES-14 cultivar, the decrease in root length might be attributed to less tolerance of this cultivar compared to the Dağdaş cultivar (Table 1). As for the Dağdaş cultivar, only the increases observed in 150 mM NaCl and 150 mM NaCl+1 mM Si treatments can be considered to be important (Table 1). Significant differences were obtained between the wheat cultivars in terms of dry weight in salt-silicone treatments ($p \leq 0.05$). The wheat silicon decreases are consistent with the results obtained by Rohanipoor et al. (2013) in corn under salt stress and the results obtained by Öncel & Keles (2002) in the wheat exposed to salt stress.

Discussions

In wheat-salt interaction, the difference detected in both wheat cultivars was found to be significant at $p \leq 0.05$ level (Table 1). In salt silicon treatment in both wheat cultivars analyzed, the difference in the root dry weight was found to be significant at $p \leq 0.05$ level (Table 1). The difference found in wheat, silicon and salt interaction was at $p \leq 0.05$ level (Table. 1). In the Dağdaş cultivar, there were decreases in 1 mM Si, 150 mM NaCl and 200 mM NaCl treatments while an increase was

observed in 150 mM NaCl+1 mM Si treatment (Table 1). In the ES-14 cultivar, there was an almost two-fold increase in 1 mM Si treatment while a decrease was observed in 50 mM NaCl treatment (Table 1). An increase was observed in 200 mM NaCl + 1 mM Si treatment (Table 1). NaCl stress in salt treatments leads to osmotic stress by preventing water uptake in plants (Çulha & Çakırlar, 2011). The resulting osmotic stress causes a decrease in the number of cells.

In the Dağdaş cultivar, while 150 mM NaCl + 1 mM Si treatment caused an increase in root dry weight, 1 mM Si treatment resulted in a decrease (Table 1). For this cultivar, based on the fact that Si alone did not make any improvement and resulted in an improvement in 150 mM NaCl + 1 mM Si treatment, it can be concluded that the concentration value of 150 mM NaCl is a regulatory value. For the ES-14 cultivar, it was concluded that the stress of 200 mM NaCl concentration was an important threshold value for this cultivar while the treatment of Si alone caused a substantial increase (Table 1). It was determined that the differences between the shoot lengths of the seedlings of the Dağdaş and the ES-14 wheat cultivars were significant ($p \leq 0.05$) (Table 1). In the Dağdaş cultivar, decreases were observed in 150 mM NaCl and 200 mM NaCl treatments (Table 1). In the ES-14 cultivar, decreases were reported in 150 mM NaCl and 200 mM NaCl treatments, as well (Table 1). These results concerning the shoot lengths are consistent with those reported by Rahman et al. (2008) concerning wheat samples under salt stress. In our study, significant differences were found in both cultivars in wheat Si, wheat NaCl and wheat Si+NaCl interactions ($p \leq 0.05$, Table 1). In the Dağdaş cultivar, increases were observed in 1 mM Si and 200 mM NaCl + 1 mM Si treatments (Table 1). These results are consistent with those reported by Rohanipoor et al. (2013) in the study where increases were observed in the shoot lengths of corns under salt stress as well as increases obtained with Si treatment. In 150 mM NaCl and 200 mM NaCl treatments, decreases were observed in comparison to the control group (Table 1). The increase observed in 200 mM NaCl + 1 mM Si treatment is greater than that obtained in 150 mM NaCl + 1 mM Si treatment, and this shows that Si made a greater impact on the shoot dry weight in 200 mM NaCl concentration (Table 1). Decreases were observed in the shoot dry weights in all groups of the ES-14 cultivar after NaCl treatment and Si made a curative effect in 200 mM NaCl concentration, and this shows that 200 mM NaCl concentration is a significant concentration value (Table 1). It is considered that studying the intermediate values between 200 mM NaCl and 150 mM NaCl concentrations is highly important.

In this study, the difference between the average root lengths of the Dağdaş and the ES-14 cultivars was found to be significant ($p \leq 0,05$). Significance of the interaction between wheat and salt might be attributed to the difference between salt tolerance levels of two cultivars. Likewise, the difference between the wheat shoot lengths was significant. It can be concluded that the Dağdaş cultivar, which is a more durable wheat genotype, and the ES-14 cultivar, which is more fragile, did not react to the same stress at the same level.

In this study, a substantial decrease was observed in the average root dry weight of the Dağdaş cultivar in 1 mM Si treatment while an increase was observed in 150 mM salt + 1 mM Si

treatment when compared to the control group. In ES-14 cultivar, a two-fold increase was detected in 1 mM Si treatment in comparison to the control group. While there were increases in 150 mM salt and 150 mM salt+1 mM Si treatments when compared to the control group, increases were observed in 200 mM salt and 200 mM salt+1 mM Si treatment, as well. In the ES-14 cultivar, it can be concluded that 200 mM salt concentration was a critical value in salt tolerance.

Acknowledgements

This study part of the MSc theses of Mehmet Hanifi Akgün.

Author Contributions

M.H.A. and N.E. performed all the experiments and drafted the main manuscript text. M.H.A. and N.E. designed the experimental work, final versions of statistics table. N.E. reviewed and approved the final version of the manuscript.

Conflict of Interest

The authors declared that no conflict of interest.

References

- Ali, A., Basra, S. M., Iqbal, J., Hussain, S., Subhani, M. N., Sarwar, M., & Ahmed, M. (2012). Augmenting the salt tolerance in wheat (*Triticum aestivum*) through exogenously applied silicon. *African Journal of Biotechnology*, 11,642-649. <http://dx.doi.org/10.5897/AJB11.3220>.
- Arnon, D. I., & Hoagland, D. R. (1940). Crop production in artificial culture solutions and in soils with special reference to factors influencing yields and absorption of inorganic nutrients. *Soil Science*, 50, 463-485.
- Çulha, Ş., & Çakırlar, H. (2011). Tuzluluğun bitkiler üzerine etkileri ve tuz tolerans mekanizmaları. *Afyon Kocatepe Üniversitesi Fen ve Mühendislik Bilimleri Dergisi*, 11(2), 11-34.
- Ediga, A., Hemalatha, S., & Meriga, B. (2013). Effect of salinity stress on antioxidant defence system of two-finger millet cultivars (*Eleusine coracana* (L.) Gaertn) differing in their sensitivity. *Advances in Biological Research*, 7,180-187. <http://dx.doi.org/10.5829/idosi.abr.2013.7.5.1113>.
- Farooq, M. A., Saqib, Z. A., Akhtar, J., Bakhat, H. F., Pasala, R. K., & Dietz, K. J. (2019). Protective role of silicon (Si) against combined stress of salinity and boron (B) toxicity by improving antioxidant enzymes activity in rice. *Silicon*, 11(4),2193-2197. <http://dx.doi.org/10.1007/s12633-015-9346-z>.

- Guo, W., Han, X., Zhang, Y., Shi, C., Zhang, H., Lin, Q., & Liu, Y. (2021). Effects of salt stress on absorption and distribution of osmotic ions in wheat seedlings. *Bangladesh Journal of Botany*, 50 (4), 1209-1214. <https://doi.org/10.3329/bjb.v50i4.57091>.
- Hu Y., & Schmidhalter, U. (2005). Drought and salinity: a comparison of their effects on the mineral nutrition of plants. *Journal of Plant Nutrition and Soil Science*, 168, 541-549. <https://doi.org/10.1002/jpln.200420516>.
- Javaid, T., Farooq, M. A., Saqib, Z. A., Akhtar, J., & Anwar-ul-Haq, M. (2019). Silicon nutrition improves the growth of salt-stressed wheat by modulating flows and partitioning of Na⁺, Cl⁻ and mineral ions. *Plant Physiology and Biochemistry*, 141, 291-299. <https://doi.org/10.1016/j.plaphy.2019.06.010>.
- Kahrizi, S., Sedghi, M., & O Sofalian, O. (2012). Effect of salt stress on proline and activity of antioxidant enzymes in ten durum wheat cultivars. *Annals of Biological Research*, 3(8), 3870-3874.
- Kardoni, F. S., Mosavi, J.S., Parande, S., & Jalil, S. (2013). Effect of salinity stress and silicon application on yield and component yield of faba bean (*Vicia faba*). *International Journal of Agricultural Science*, 6(12),814-818.
- Liang, Y., Sun, W., Zhu, Y. G., & Christie, P. (2006). Mechanisms of silicon-mediated alleviation of abiotic stresses in higher plants: a review. *Environmental Pollution*, 147(2), 422-428. <https://doi.org/10.1016/j.envpol.2006.06.008>.
- Öncel, I., & Keleş, Y. (2002). Tuz stresi altındaki buğday genotiplerinde büyüme, pigment içeriği ve çözümlü madde kompozisyonunda değişimler. *Cumhuriyet Üniversitesi Fen Fakültesi Fen Bilimleri Dergisi*, 23(2).
- Rahman, M., Soomro, U. A., Haq, M. Z. U., & Gul, S. H. (2008). Effects of NaCl salinity on wheat (*Triticum aestivum* L.) cultivars. *World Journal of Agricultural Sciences*, 4(3), 398-403.
- Reichert, E. T., Wilson, J. P., McGlynn, S. E., & Fischer, W. W. (2015). Four hundred million years of silica biomineralization in land plants. *PNAS*, 112(17),5449-5454. <https://doi.org/10.1073/pnas.1500289112>.
- Rohanipoor, A., Norouzi, M., Moezzi, A., & Hassibi, P. (2013). Effect of silicon on some physiological properties of maize (*Zea mays*) under salt stress. *Journal of Biological & Environmental Sciences*, 7(20), 71-79.
- Rubio, M. I., Escrig, I., Martinez-Cortina, C., Lopez-Benet, F. J., & Sanz, A. (1994). Cadmium and nickel accumulation in rice plants. Effects on mineral nutrition and possible interactions of

abscisic and gibberellic acids. *Plant Growth Regulation*, 14(2),151-157.
<https://doi.org/10.1007/BF00025217>.



Capture of a Rare Smoothback Angelshark *Squatina oculata* (Squatinidae) in Turkish Waters, with Updated Records from the eastern Mediterranean Sea

Okan Akyol ^{1*} , Tülin Çoker ² , H. Betül Toprak ³ , Christian Capapé ⁴ 

¹ Ege University Faculty of Fisheries, 35440 Urla, İzmir, Türkiye.

² Muğla Sıtkı Koçman University Faculty of Fisheries, 48000 Muğla, Türkiye.

³ Marmaris Directorate of the Ministry of Agriculture and Forestry, Muğla, Türkiye.

⁴ Université de Montpellier, Laboratoire d'Ichtyologie, 34 095 Montpellier cedex 5, France.

Abstract

The authors report on the capture of a specimen of smoothback angelshark *Squatina oculata* Bonaparte, 1840 from Turkish marine waters. The specimen measured 720 mm in total length and was caught by means of a commercial purse-seiner at a depth of 60 m. The species appeared to be sporadically caught in the area and the eastern Mediterranean Sea, however, the size diversity of recorded specimens shows the species still occurred in the region. Although the smoothback angel shark is listed as a protected species according to Turkish Marine Fisheries Act, a management plan should be integrated with local fisheries to preserve the species from extirpation throughout its distribution range in Turkish seas.

Keywords:

Squatinidae, fishing pressure, management, threatened species, eastern Mediterranean Sea

Article history:

Received 14 December 2022, Accepted 15 February 2023, Available online 10 April 2023

Introduction

Smoothback angelshark *Squatina oculata* Bonaparte, 1840 is known in the eastern Atlantic from Morocco to Angola, and it is one of the three Mediterranean species belonging to the genus *Squatina* Duméril, 1806 (Roux, 1984). *S. oculata* occurs in the western Mediterranean Basin, but the species was unknown off the Mediterranean coast of France (Capapé et al., 2000). Tortonese (1956) noted its occurrence in Italian waters, and Zava et al. (2016) collected 4 juvenile specimens from the Strait of Sicily. Zava et al. (2022) also documented 34 specimens of *S. oculata*, of which

*Corresponding Author: Okan AKYOL, E-mail: okan.akyol@ege.edu.tr

32 from the central Mediterranean Sea (21 from Malta, 6 from Tunisia, 5 from Sicily and 2 from Egypt) were incidentally captured or observed between 2005 and 2021.

Squatina oculata is also reported in the eastern Mediterranean where it was first confirmed in the Levant Basin (Golani, 1996), and furtherly from the Syrian coast (Ali, 2018) and the Lebanese coast (Bariche & Fricke, 2020) and recently, from the Egypt (Zava et al., 2022). Ergüden et al. (2019) listed findings of *S. oculata* in the entire Turkish waters where the species is sporadically caught and considered as rather rare in the region. In a recent study, Özgür Özbek & Kabasakal (2022), provided notes on the biology of *S. oculata*, based on observations of 15 specimens captured by commercial bottom-trawlers operated in the Gulf of Antalya.

The main goal of the present paper is to report the capture of a specimen of *S. oculata* together with an extensive literature review that included previous checklists, and individual species accounts from the eastern Mediterranean Sea. This information will allow us to assess in the region, the real status of *S. oculata* classified as “Critically Endangered” in the Global List by the International Union of Conservation of Nature (IUCN, 208), as the two other Mediterranean congeneric species, sawback angelshark *S. aculeata* Cuvier, 1829 and common angelshark *S. squatina* (Linnaeus, 1758).

Materials and Methods

On 1st September 2022, a specimen of *Squatina oculata* was captured by means of a commercial purse-seiner at a depth of 60 m, off Marmaris, Mugla, 36°44' N - 28°20' E (Figure 1), following information provided by fishermen. The specimen was landed at the fish market, where it was carefully observed, identified and photographed. Unfortunately, it was rapidly cut into slices and sold to local consumers. Therefore, no morphometric measurements could be taken.

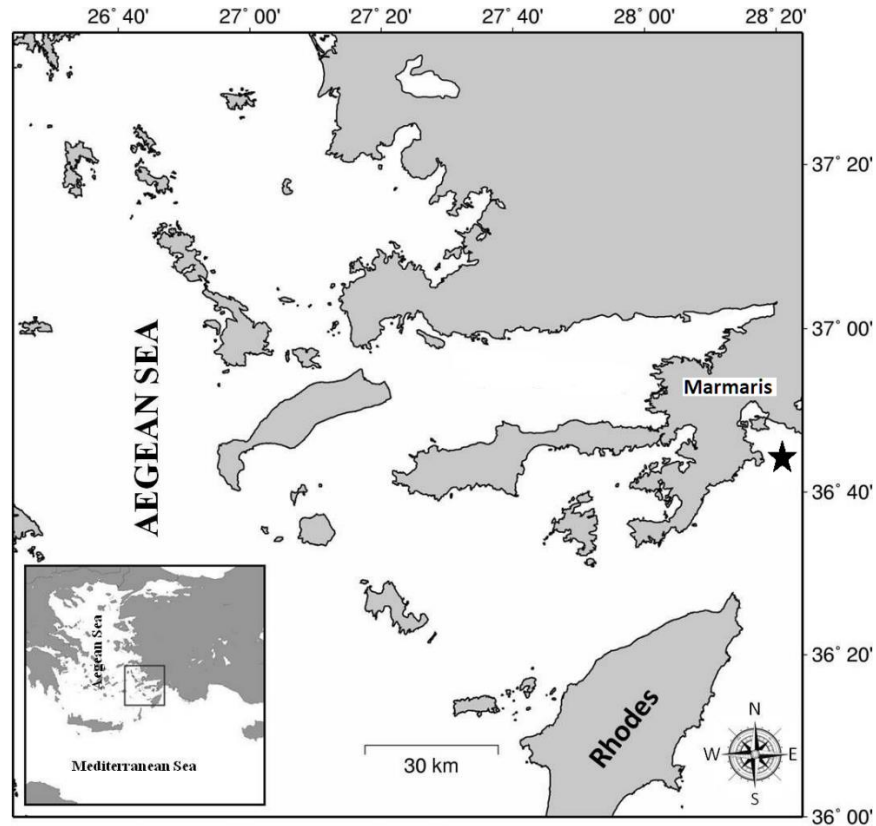


Figure 1. Map indicating the capture site (black star) of *Squatina oculata*, off Marmaris, in the Aegean Sea

Results and Discussion

The examined specimen was a female measuring 720 mm in total length (Figure 2). It was identified as *Squatina oculata* via based on the combination of main morphological characteristics: trunk very broad, eye diameter equal to or larger than spiracle length; external nasal flap with two barbels bordering a fringed median lobe (Figure 3A, 1); dermal folds on sides of head slightly undulate (Figure 3A, 2); pectoral fins very high and broad with broadly rounded rear tips; hind tips of pelvic fins not reaching the level of first dorsal fin origin, dorsal surface rough but no median line of spines, lower surface with small denticles only on the front margin of pectoral and pelvic fins and down the centre of tail; teeth pointed, slightly curved at the distal end and with a triangular base, dispersed in 20/20 in upper and lower jaws (Figure 3 B, 3), colour greyish-brown with some white spots, and belly beige. The description and colour of the present specimen are coincided with the descriptive characteristics provided in Roux (1986), Capapé & Roux (1980), Compagno (1984), Kabasakal & Kabasakal (2004), Ergüden et al. (2019) and Rafrafi-Nouira et al. (2022).



Figure 2. *Squatina oculata*, captured off Marmaris, SE Aegean Sea, scale bar = 50 mm (Photo: H.B. Toprak)

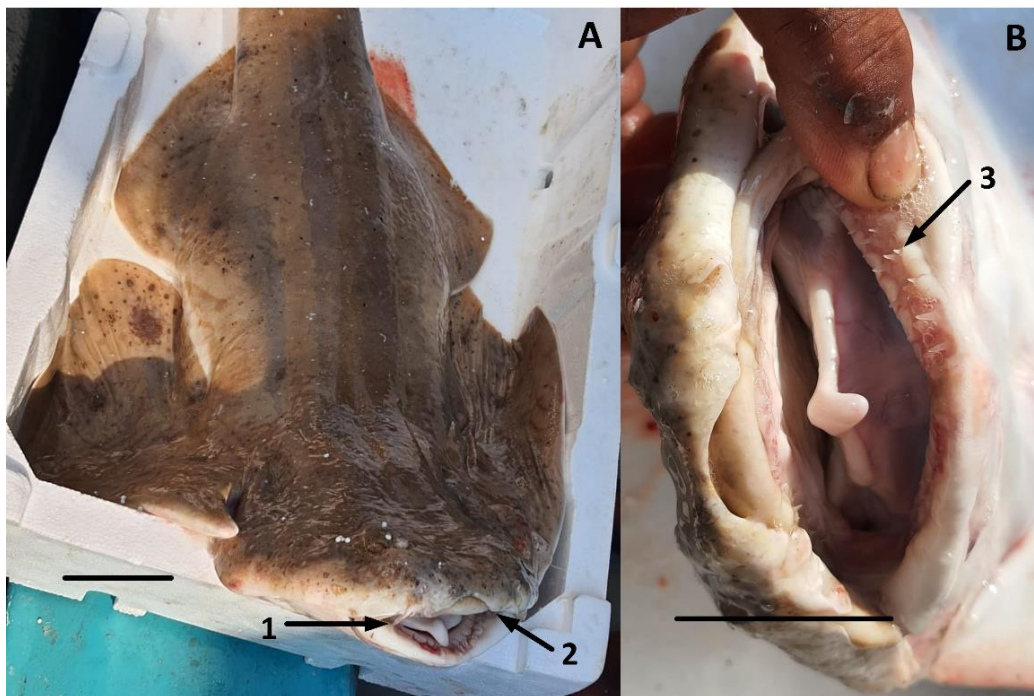


Figure 3. *Squatina oculata*, captured off Marmaris, SE Aegean Sea. A) Front of the head showing, (1) barbels bordering a fringed median lobe, (2) dermal folds on sides of head slightly undulate, scale bar = 50 mm. B) Opening of the mouth showing teeth (3), scale bar = 100 mm (Photo: H.B. Toprak)

Recent captures of *S. oculata* in the eastern Mediterranean Sea, where the species appeared to be sporadically caught mostly as solitary specimens, are listed in Table 1. The nature of the solitary occurrence of *S. oculata*, which was suggested by the previous observation of Kabasakal & Kabasakal (2004) and Ergüden et al. (2019) was also confirmed with present specimen. *S. oculata* has a high economic value and is threatened by fishing pressure due to its K-selected characteristics (Capapé et al., 1990). Furthermore, smoothback angel shark is considered under the threat of multimodal fisheries in Turkish waters (Ergüden et al., 2019; Kabasakal, 2021), The specimens included in Table 1 show the occurrence of specimens displaying different sizes, showing that the species has not totally disappeared in the region. However, they do not constitute sufficient records allowing to suggest that a viable population is really established.

Table 1. Contemporary records of *Squatina oculata* from the eastern Mediterranean

Location	Depth (m)	Gear*	Record date	Number collected	Size, TL (mm)	References
Haifa, Israel E Mediterranean	30-100	BT	11 Mar.1990	1	612	Golani (1996)
Erdek Bay, the Sea of Marmara	31	BT	17 Apr.1992	1	294	Meriç (1994)
Off Karataş, NE Mediterranean	50-60	BT	1994-1996	1	756	Başusta & Erdem (2000)
Gökçeada, NE Aegean Sea	?	BT	July 1997	1	300	Kabasakal & Kabasakal (2004)
Gökçeada, NE Aegean Sea	?	BT	Sept.1999	1	950	Kabasakal & Kabasakal (2004)
NW Rhodes, Greek Aegean Sea	60-80	BT	23 Dec.2004	1	795	Corsini & Zava (2007)
Gulf of Antalya, NE Med.	50-100	BT	2009-2010	10	240-880	Özgür Özbek & Kabasakal (2022)
Gulf of Antalya, NE Med.	10-200	BT	2009-2011	13	482-804	Mutlu et al. (2022)
Coast of Egypt	?	?	?	?	?	El Sayed et al. (2017)
Aydıncık, NE Mediterranean	65	BT	4 Nov.2017	1	726	Ergüden et al. (2019)
Coast of Syria	?	?	?	?	?	Ali (2018)
Gökçeada, NE Aegean Sea	110	BT	22 Mar.2018	1	875	Yığın et al. (2019)
Tyre, Lebanon, E Mediterranean	?	?	10 Apr.2019	1	?	Bariche & Fricke (2020)
Off El-Hamam, Egypt	55-70	BT	28 Mar.2021	2	492-700	Zava et al. (2022)
Off Marmaris, SE Aegean Sea	60	PS	01 Sept. 2022	1	720	This study

*BT: Bottom trawl; PS: Purse seine

Similar patterns were observed for squatid species from the Tunisian coast, which have an important commercial interest for local fisheries (Capapé et al., 1990; 2002). In total accordance with Ergüden et al. (2019) and Kabasakal (2021), a management plan should be integrated with the local fisheries together with the contribution of local fishermen. It should be essential to preserve the squatid species from their extirpation throughout the areas where they habitually aggregated.

Author Contributions

OA; Writing - original draft, visualization, writing – review & editing. TÇ; Investigation, interview, HBT; Data collection, interview and take photographs. CC; Conceptualization, methodology, writing - original draft, writing - review & editing.

Conflict of Interest

The authors declare that there are no conflicts of interest.

Data Availability Statement

The data supporting this study's findings are available on request from the corresponding author OA.

Compliance with Ethical Standards

Local Ethics Committee Approval was not obtained because experimental animals were not used in this study.

References

- Ali, M. (2018). An updated checklist of marine fishes from Syria with an emphasis on alien species. *Mediterranean Marine Science*, 19(2), 388-393. <https://doi.org/10.12681/mms.15850>.
- Bariche, M. & Fricke, R. (2020). The marine ichthyofauna of Lebanon: an annotated checklist, history, biogeography and conservation status. *Zootaxa*, 4775(1), 1-157. <https://doi.org/10.11646/zootaxa.4775.1.1>.
- Basusta, N. & Erdem, Ü (2000). A study on the pelagic and demersal fishes of Iskenderun Bay. *Turkish Journal of Zoology*, 24 (Suppl.), 1-19. (in Turkish).
- Capapé, C. & Roux C. (1980). Etude anatomique des ptérygiopodes des Squatinidæ (Pisces, Pleurotremata) des côtes tunisiennes. *Bulletin du Muséum national d' Histoire naturelle de Paris*, 4 ème série, 2ème section A, 4, 1161-1180.
- Capapé, C., Quignard J.P. & Mellinger J. (1990). Reproduction and development of two angel sharks, *Squatina squatina* and *S. oculata* (Pisces: Squatinidæ), off Tunisian coasts: semi-delayed vitellogenesis, lack of egg-capsules and lecithotrophy. *Journal of Fish Biology*, 37(3), 347-356. <https://doi.org/10.1111/j.1095-8649.1990tb0565.x>.
- Capapé, C., Tomasini J.A. & Quignard J.-P. (2000). Les Elasmobranches Pleurotrèmes de la côte du Languedoc (France méridionale, Méditerranée septentrionale). Observations biologiques et démographiques. *Vie et Milieu*, 50(2), 123-133.
- Capapé, C., Seck A.A., Gueye-Ndiaye A., Diatta Y., & Diop M. (2002). Reproductive biology of the smoothback angelshark, *Squatina oculata* (Elasmobranchii: Squatinidae), from the coast

of Senegal (eastern tropical Atlantic). *Journal of the Marine Biological Association of the United Kingdom*, 82(4), 635-640. <https://doi.org/10.1017/S0025315402005994>.

Compagno, L.V.J. (1984). FAO species catalogue. Vol 4. Sharks of the world. An annotated and illustrated catalogue of sharks species known to date. Part 2. Carcharhiniformes. FAO Fish. Syn. (125), Part 1., FAO, Rome, pp. 1-269.

Corsini, M. & Zava, B. (2007). Recent capture of *Squatina oculata* and *Squatina oculata* from Dodecanese Islands (SE Aegean Sea, Eastern Mediterranean). *Biologia Marina Mediterranea*, 14(2), 352-353.

Ergüden, D., Ayas, D., Gürlek, M., Karan, S. & Turan, C. (2019). First documented smoothback angelshark *Squatina oculata* Bonaparte, 1840 from the North-Eastern Mediterranean Sea, Turkey. *Cahiers de Biologie Marine*, 60(2), 189-194. <https://doi.org/10.21411/CBM.A.23607FF9>.

El Sayed, H., Akel K. & Karachle P.K. (2017). The marine ichthyofauna of Egypt. *Egyptian Journal of Aquatic Biology and Fisheries*, 21 (3), 81-116. <https://doi.org/10.21608/ejabf.2017.4130>.

Golani, D. (1996). The marine ichthyofauna of the eastern Levant-History, inventory and characterization. *Israel Journal of Zoology*, 42, 15-55.

IUCN, (2018). The IUCN Red List of Threatened Species. Version 2017-3. (<http://www.iucnredlist.org>). Accessed on 25 November 2022.

Kabasakal, H. (2003). Historical and contemporary records of sharks from the Sea of Marmara, Turkey. *Annales, Series Historia Naturalis*, 13(1), 1–12.

Kabasakal, H. (2021). Chapters from life history of common angel shark *Squatina squatina*, from Turkish waters: a historical, ethnoichthyological and contemporary approach to a little-known shark species. *Journal of the Black Sea/ Mediterranean Environment*, 27(3), 317-341.

Kabasakal, H. & Kabasakal, E. (2004). Sharks captured by commercial fishing vessels off the coasts of Turkey in the Northern Aegean Sea. *Annales, Series Historia Naturalis*, 14(2), 171-180.

Meriç, N. (1994). Some uncommon fishes from the Turkish seas. XII. Ulusal Biyoloji Kongresi, Trakya Üniversitesi, Edirne, 6–8 July 1994, Bildiriler Kitabı. Edirne, pp. 295–299. [in Turkish]

- Mutlu, E., Deval, M. C., Miglietta, C., Saygu, I. & de Meo, I. (2022). Biometrical distribution of sharks in a low Elasmobranchs-diversified shelf, the eastern Mediterranean Sea. *Acta Biologica Turcica*, 35(2), A2, 1-22.
- Özgür Özbek, E. & Kabasakal H. (2022). Notes on smoothback angel shark, *Squatina oculata* (Squatiniformes: Squatinidae) caught in the Gulf of Antalya. *Annales, Series Historia Naturalis*, 32, 9-16.
- Rafrafi-Nouira, S., Chérif, M., Reynayd, C. & Capapé C. (2022). Captures of the rare smoothback angelshark *Squatina oculata* (Squatinidae) from the Tunisian coast (Central Mediterranean Sea). *Thalassia Salentina*, 44, 3-8. <https://doi.org/10.1285/i15910725v44p3>.
- Roux, C. (1984). Squatinidae. pp. 148-150. In: P.J.P. Whitehead., M.-L. Bauchot, J.-C. Hureau, J. Nielsen & E. Tortonese, (Eds.). Fishes of the north-eastern Atlantic and the Mediterranean. UNESCO, Paris.
- Tortonese, E. (1956). Leptocardia, Ciclostomata, Selachii. In: Fauna d'Italia. Calderini, Bologna. vol.2, 334 p.
- Yığın, C.Ç., İşmen, A., Daban, B., Cabbar, K. & Önal, U. (2019). Recent findings of rare sharks, *Squatina oculata* Bonaparte, 1840 and *Squatina squatina* (Linnaeus, 1758) from Gökçeada Island, Northern Aegean Sea, Turkey. *Journal of the Black Sea/Mediterranean Environment*, 25(3), 305-314.
- Zava, R., Fiorentino F. & Serena F. (2016). Occurrence of juveniles *Squatina oculata* Bonaparte, 1840 (Elasmobranchii: Squatinidae) in the Strait of Sicily (Central Mediterranean). *Cybium*, 40(4), 341-343.
- Zava, B., Insacco, G., Deidun, A., Said, A., Ben Souissi, J., Nour, O.M., Kondylatos, G., Scannella, D. & Corsini-Foka, M. (2022) Records of the critically endangered *Squatina aculeata* and *Squatina oculata* (Elasmobranchii: Squatiniformes: Squatinidae) from the Mediterranean Sea. *Acta Ichthyologica et Piscatoria*, 52(4), 285–297. <https://doi.org/10.3897/aiep.52.94694>.



Morphological Description of Megalopal Stages of Three Portunid Species (Decapoda, Brachyura, Portunidae) from Indus Deltaic Area (northern-Arabian Sea)

Urwah Inam ^{1*} , Qadeer Mohammad Ali ¹ , Quratulan Ahmed ¹ , Levent Bat ² 

¹ The Marine Reference Collection and Resources Centre, University of Karachi, Karachi-75270, Pakistan

² Sinop University, Fisheries Faculty, Department of Hydrobiology, 57000, Sinop, Türkiye

Abstract

The larvae of crustaceans, including those of brachyuran crabs, are a significant part of zooplanktonic communities constituting an ecologically important fraction of the pelagic communities. The present study describes taxonomic studies on three megalop stages of *Portunus pelagicus* (Linnaeus, 1758), *Charybdis feriatus* (Linnaeus, 1758) and *Carcinus maenas* (Linnaeus, 1758) belonging to family Portunidae collected from Indus deltaic creek system. Zooplankton samples were collected from three locations: Shahbandar 24°15'48.083'N, 67°90'15'333'E, Ketibandar 24°9'16.06'N, 67°27'7.64'E and Korangi creek 24°48'18.80''N, 67°12'30.31'E during April to October 2018. No data available on taxonomic studies of portunid megalops upto species level from Paksitan, hence this is a first attempt to examine and to describe taxonomic features of megalops collected in the zooplankton samples. This study will contribute to the scientific knowledge on megalops taxonomy and identification as well as be useful for future research by taxonomists and biologists.

Keywords:

Megalops, taxonomic features, portunid species, Indus deltaic area

Article history:

Received 25 December 2022, Accepted 14 March 2023, Available online 10 April 2023

Introduction

The megalopa is transitional stage between planktonic zoea and the benthic adults which is morphologically unique phase in the life cycle of crab. A larval stage following the zoea in the

*Corresponding Author: Urwah INAM, E-mail: utssinam@gmail.com

development of most crabs in which the legs and abdominal appendages have appeared, the abdomen is relatively long, and the eyes are large called megalops. The larvae of crustaceans, including those of brachyuran crabs, are a significant part of zooplanktonic communities, constituting an ecologically important fraction of the pelagic communities. The zooplanktons are important component of an aquatic food web by forming link in the trophic level as secondary producers. The study of brachyuran crab larvae has many useful applications, such as dispersal and recruitment studies, possible depletion of species vulnerable to over exploration (Clark & Paula, 2003), evaluating a species diversity in a region and in specifying the reproduction time of brachyuran species (Kornienko & Korn, 2009), systematics, analyses of physiological ecology and analysis of larval behaviour (Hines, 1986). There are over 4500 species of crab in the world, more than 200 crab species have been documented from Pakistani waters, out of which just five are edible (Kazmi, 2003; Kalhor, 2018) *Portunus pelagicus* (Linnaeus, 1785) and *Portunus sanguinolentus* (Herbst, 1783) are most dominant species from Pakistan and others are *Scylla tranquebarica* (Fabricius, 1798), *S. olivacea* (Herbst, 1796) and *Charybdis feriatus* (Linnaeus, 1785). *Portunus pelagicus*, *Charybdis feriatus*, *Carcinus maenas* are portunid crab belonging to family Portunidae. This group known as swimming crabs and they are characterized by the flattening of the fifth pair of legs into wide paddles, which are used for swimming, this capability, together with their strong, sharp claws, allows many species to be fast and aggressive predators (Davie, 2002). The swimming crabs (family Portunidae) are distributed worldwide and commonly inhabit estuaries, mangroves, reefs, shallow and the deep sea (Huang & Shih, 2021). *P. pelagicus* distributed throughout the Indo-West Pacific and contribute and important fishery and plays an important role in different regions (Stephenson, 1962; Potter et al., 1983; Kailola et al., 1993; Bryars & Havenhand, 2004).

The coastal region of Sindh lies in the southeast of the country between the Indian border along the Sir creek in the east to the Hub river along the coast of Balochistan in the west. The Sindh coast can be further divided into two parts, the Sindh coast covering 85 % of the coastal belt, whose coastal morphological features among tidal flats; delta wet-lands; estuarine systems and a broad flat continental ledge. The Indus river is ranked as the 22nd largest river on the globe and has developed a fan-shaped delta that is one of the largest bodies of sediment in the modern ocean basins. The Indus delta is the sixth largest delta on the earth with an area of 29.524 km². The present delta includes 17 major creeks characterized by mangrove forests; tidal flats; salt marshes and sand dunes, and 97 % of the total mangrove cover in Pakistan is represented by the Indus delta comprising about 95 % almost monotypic dominant species *Avicennia marina* (Ali & Ahmed, 2013). The Indus delta is a home of the largest arid zone mangrove forest in the world, stretching from Korangi creek in the west to Sir creek in the east. The Indus river forms an extensive system of streams, riverbeds, tidal flats, swamps, estuaries and mangrove forests. These streams represent a delicate ecosystem that provides shelter and food for a variety of marine organisms, including commercially important fish and shellfish (Ali & Ahmed, 2014). This creek system is nutrient affluent and providing breeding ground and nursery for a spacious diversity of organisms. The

mangrove ecosystem has been familiar as an unbelievable likely resource for its environmental and biological dynamism. Its performing a vital role in fisheries and coastal safety as a usual fence alongside hurricanes and storms.

Earlier published literatures are available on the taxonomic and larval composition of brachyuran crabs from Pakistani coastal waters studied by (Hashmi 1969; 1970a,b; Siddiqui & Tirmizi, 1992; Tirmizi et al., 1993 Ghory & Siddiqui, 2000; Ghory, 2002; Ghory & Siddiqui, 2006; Ghory & Siddiqui, 2008; Ghory et al., 2018). The aim of the present study megalopal stages were isolated from the zooplankton samples collected for identification and taxonomic studies from three major creeks (Shahbandar, Ketibander and Korangi creeks) Indus deltaic area during April to October 2018. The data will be a good addition to the scientific knowledge on taxonomy and identification of megalops and it will also be helpful for taxonomists and biologists for future research.

Materials and Methods

The megalopal stages were sorted out from zooplankton samples collected from three designated sites in Indus deltaic area (Shahbandar 24°15'48.083'N, 67°90'15'333'E), Ketibandar (24°9'16.06'N,67°27'7.64'E) and Korangi (24°48'18.80''N,67°12'30.31'E) during April to October 2018 (Figure 1). Physico-chemical parameters such as water temperature (°C); salinity (ppt), dissolved oxygen (mg/L); pH and transparency (cm) were measured. For the water temperature (°C), a glass thermometer was immersed below the water surface (10 cm) for three minutes and the measured temperature (°C) was recorded in the data sheet. The salinity (ppt) was measured using a refractometer (S/Mill-E, Atago Co. Ltd., Tokyo, Japan). Dissolved oxygen (mg/L) was measured using a portable device (OSK-14808, DO-20A). The pH was recorded using a digital portable device (model 220 Pen). The transparency (cm) of water was measured using a Secchi disk (Hydro-Bios, 443590).

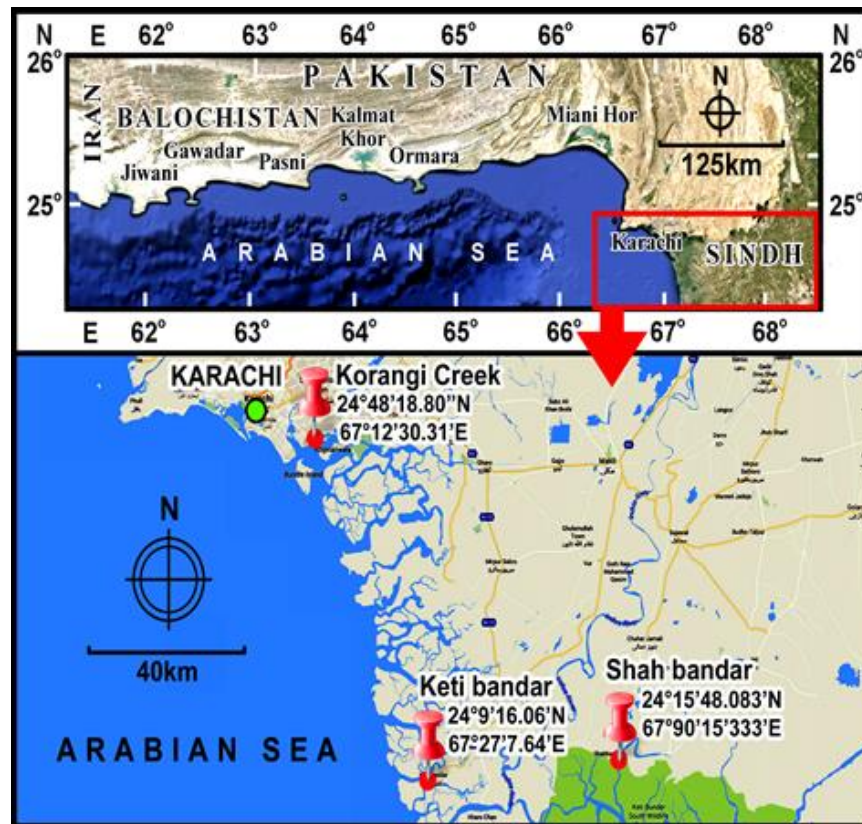


Figure 1. Map showing designated stations in the three major creeks; Shahbandar, Ketibandar, and Karangi, Indus deltaic area, northern Arabian Sea

Zooplankton samples were collected using a 500 microns mesh Hydrobios ring trawl by horizontal trawling for 10 minutes at a constant speed of 0.5 m/s from surface waters. A digital flow meter was used to measure the volume of water flowing through the net. Samples were immediately preserved in 5% (buffered formalin) and placed in plastic containers for laboratory analysis. Samples were divided into aliquots (sub-samples) and megalops were sorted out. Megalop specimen were identified and counted in a counting dish under a stereomicroscope (Wild 181300, Switzerland). Microphotography was also performed using a digital camera (Fujifilm 16 MP). Morphological features and characteristics (colour, size, carapace, abdomen, telson, antennae, mandible, maxilla, periopod, etc.) were studied. Dissection was performed under the stereo zoom microscope.

Carapace was precise from the rostrum tip to the rear edge, the carapace width, across the widest part of the carapace; Rostrum length, from apex to front part of orbit at midline; Belly length, from mid-posterior edge of carapace to tip of telson. Appendages were dissected in glycerol using entomological needles. Drawings, illustrations were made with help of drawing tubes fixed on a stereo zoom microscope (Wild 181300, Switzerland) (10x1x50 = 500x magnification). The

taxonomic studies, identification was conducted with the help of literatures (Newell & Newell, 1977; Pessani et al., 2004; Weiss, 2017).

Results

Original photographs of the species are given in Figures 2.

Family-Portunidae

Portunus pelagicus (Linnaeus, 1758) (Figure 2A)

Material Examined: Location: Shahbandar, Korangi; No. of specimens: 04; Size: Total length was 2 to 2.2 mm and 1.4 to 1.6 mm width.

Diagnosics characteristics:

Carapace (Figure 3A, B): Rectangular and no dorsal or lateral spines present, rostral spine presents half of the length of antenna.

Antennule (Figure 3C): 3-segmented peduncle; unsegmented endopod and five-segmented exopod. aesthetasc setae on outer margin; terminal segment has two stiff simple setae, one terminally and the other sub-terminally.

Antenna (Figure 3D): uniramous, with more than 12-13-segments; no setae present on proximal segment.

Mandible (Figure 3E): Segmented coxalendite, unsegmented basal endite; 2-segmented, endopod.

Maxillula (Figure 3F): Segmented coxalendite, unsegmented basal endite and 2-segmented endopod.

Maxilla (Figure 3G): Endopod two segmented, proximal segment with three setae, distal segment without setae, scaphognathite with several plumose setae.

First maxilliped (Figure 3H): Epipod with 5 setae, coxa and basis unsegmented with several setae, endopod unsegmented with 5 setae, exopod 3-segmented, distal segment with 5 setae.

Second maxilliped (Figure 3I): Endopod four segmented; exopod five segmented, distal segment with four setae.

Third maxilliped (Figure 3J): Exopod two segmented, distal segment with four setae; epipod unsegmented with few plumodenticulate setae and gills.

First periopod (Figure 3K): Well developed. Few short setae on all segments.

Second and fifth pereopods (Figure 3L, M): Well developed with four segmented endopods.

Pleopod (Figure 3N): Exopods bear plumose setae.

Telson (Figure 3O): It is dorso-ventrally flattened.

Charybdis feriatus (Linnaeus, 1758) (Figure 2B)

Material Examined: Location: Ketibandar; No. of specimens: 03; Size: Total length was 1.4 to 1.5 mm and 0.9 to 1 mm width.

Diagnosics Characteristics:

Carapace (Figure 4A): Carapace broad, rostrum short and knob like.

Antennule (Figure 4B): 3 segmented peduncle, expanded proximal segment, 2 distal flagella present. endopod with three setae; exopod with 19 aesthetascs and 1 seta.

Antenna (Figure 4C): Endopod elongated and multisegmented flagellum.

Maxillula (Figure 4D): Coxalendite with plumodenticulate setae.

Maxilla (Figure 4E): Coxal endite uniramous with 7 plumodenticulate setae, basal endite bilobed with 9+ 11 setae, endopod unsegmented, exopod (scaphognathite) with several setae. Coxal and basal endites both are bilobed.

Maxilliped (Figures 4F, G, H): maxilliped 1 has epipodhas 21 setae, exopod has 2,5 setae.

Maxilliped 2: protopod 1 setae, endopod 2,3,2,8,10 setae, exopod 1.6 setae.

Pereopod (Figures 4I, J): A couple of huge cornua found inposterior-laterally on sternal shield.

Telson (Figure 4K): Long and broad; subsequent edging convexly curved, dorsal surface with two pairs of small setae.

Carcinus maenas (Linnaeus, 1758) (Figure 2C)

Material Examined: Location: Shahbandar, Korangi; No. of specimens: 05; Size: Total length is (1.72 to 1.75 mm) and is (0.4 to 0.5 mm) width

Diagnostic characteristics:

Carapace (Figures 5A, B): Dorsal surface of carapace with a pair of small bristles, rostrum tip pointed onward and somewhat descending. Between eyes rostrum was with skinny dejection.

Antennule (Figure 5C): Exopode 4 segmented cheliped ischial spine, or pereopod 2-coxal spine or both.

Antenna (Figure 5D): 8-segmented, and no setae found on distal end of last segment.

Maxilla (Figure 5E): Well developed.

Pereiopod (Figures 5F, G): Slightest seven segmented pereiopod; five dactyls with terminal sub terminal setae. Pereiopod five dactyl with two, three or four incurable or sub incurable setae.

Telson (Figure 5H): long and broad, dorsal surface with three pairs of small setae.

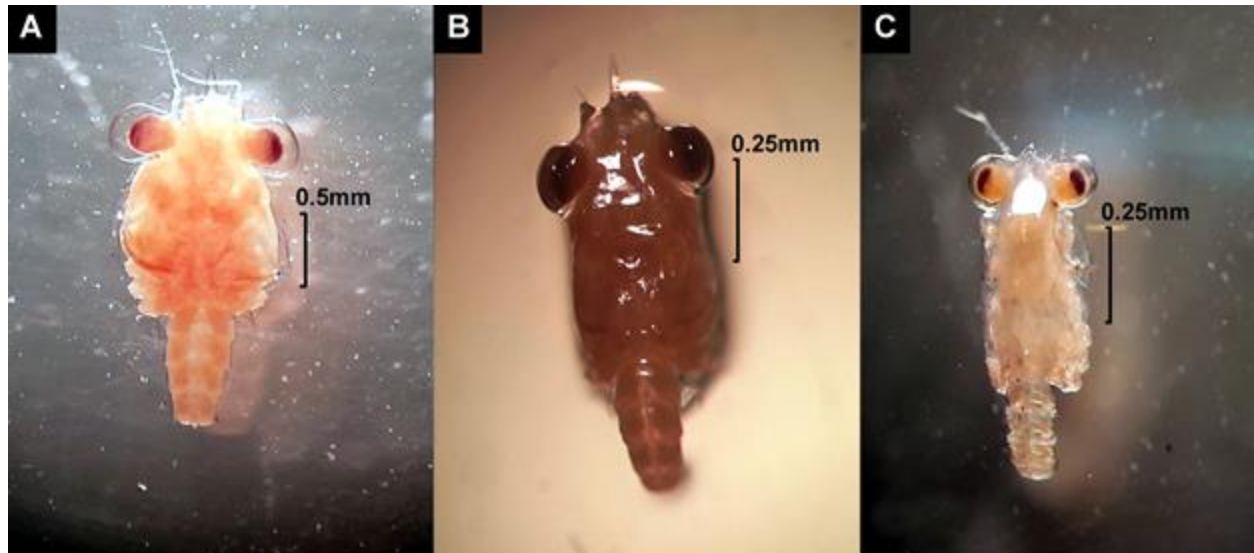


Figure 2. A) *Portunus pelagicus* (Linnaeus, 1758) B) *Charybdis feriatus* (Linnaeus, 1758) C) *Carcinus maenas* (Linnaeus, 1758)

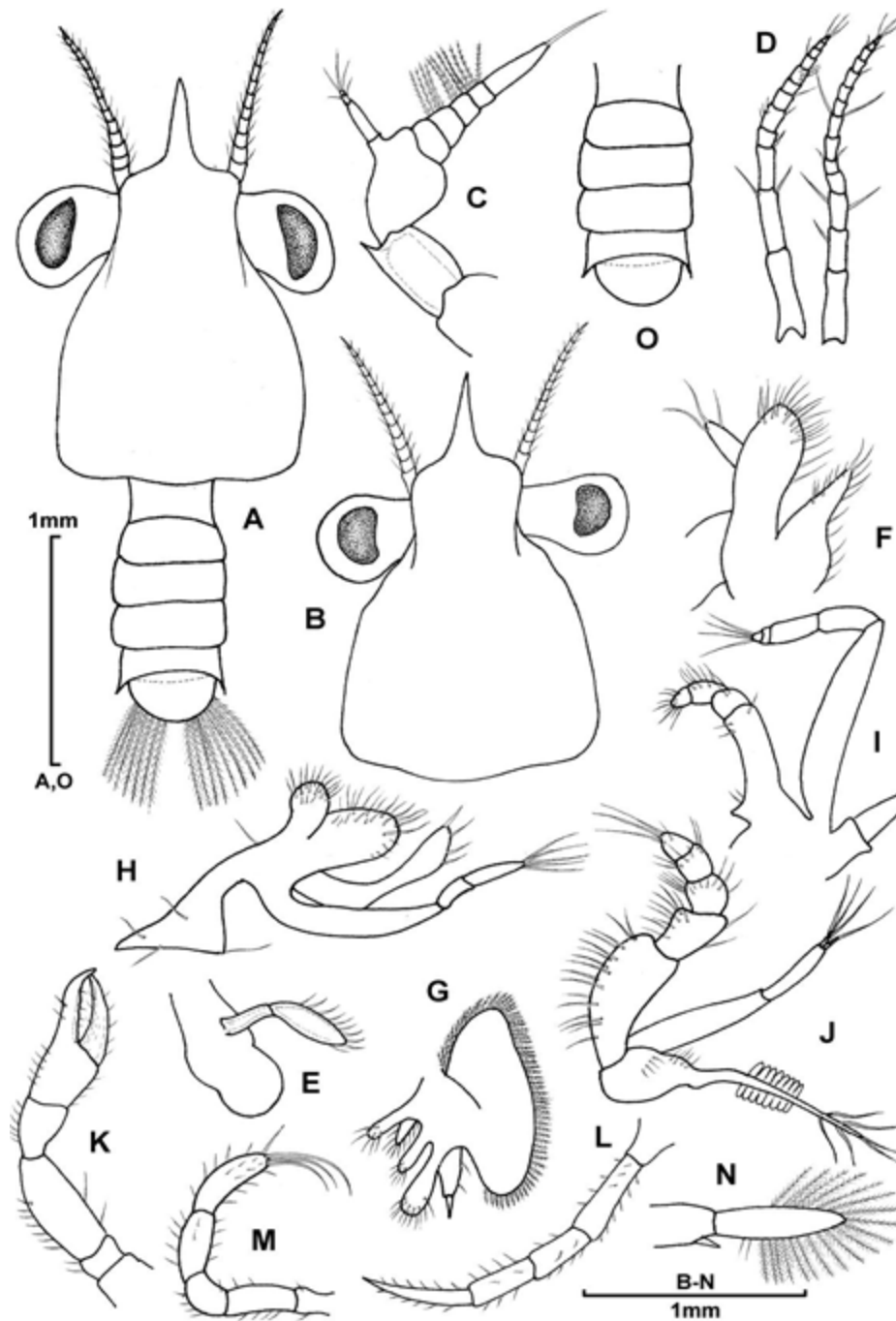


Figure 3. Taxonomy of megalopal stage of *Portunus pelagicus* A) Dorsal view B) Carapace C) Antennule D) Antenna E) Mandible F) Maxillule G) Maxilla. H) First maxilliped I) Second maxilliped J) Third maxilliped K) 1st pereopod L) Second pereopod M) Fifth pereopod N) Pleopod O) Telson.

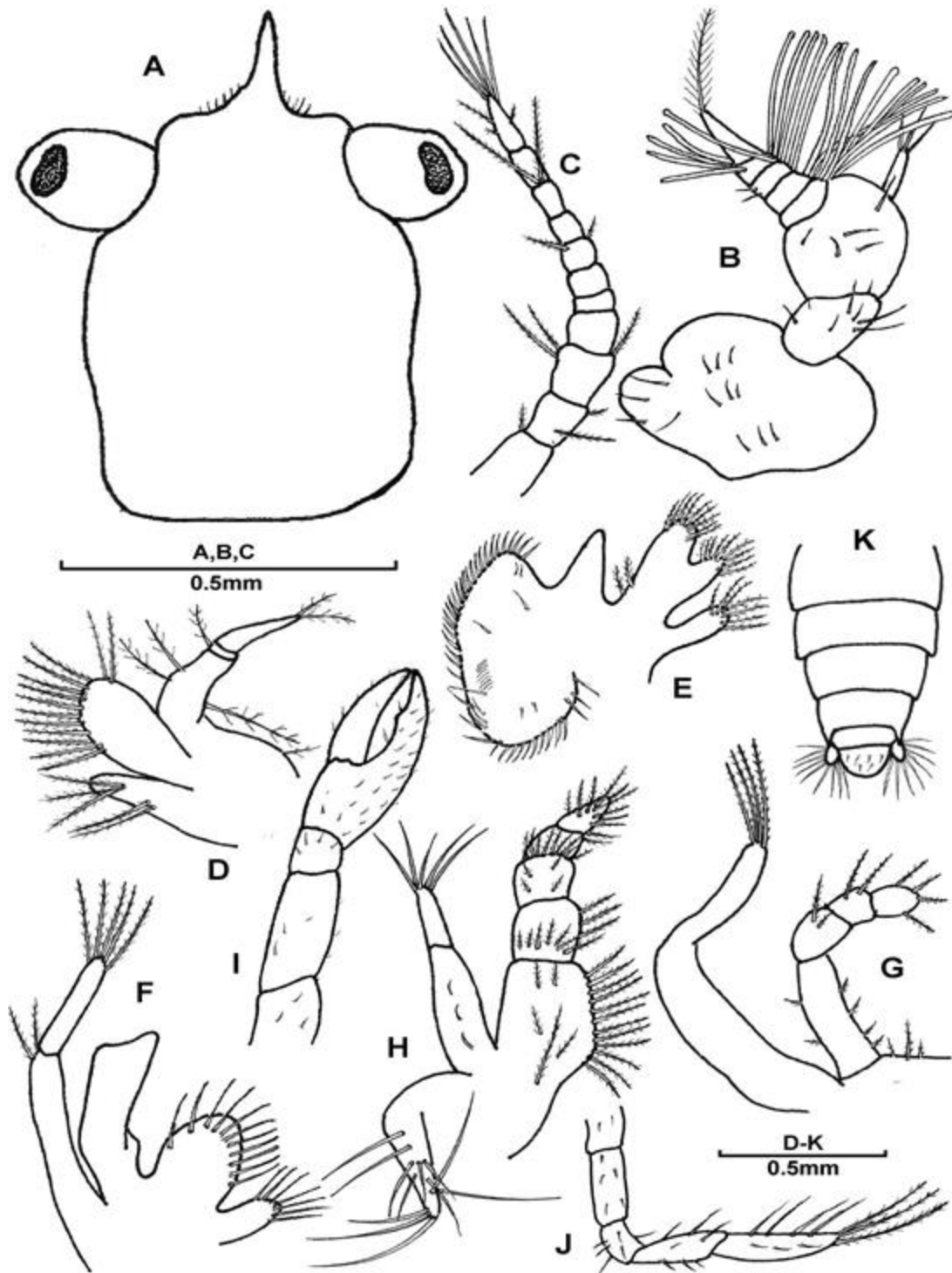


Figure 4. Taxonomy of megalopal stage of *Charybdis feriatus* A) Carapace B) Antennule C) Antenna D) Maxillule E) Maxilla F) First maxilliped G) Second maxilliped H) Third maxilliped I) First pereopod J) Fifth pereopod K) Telson

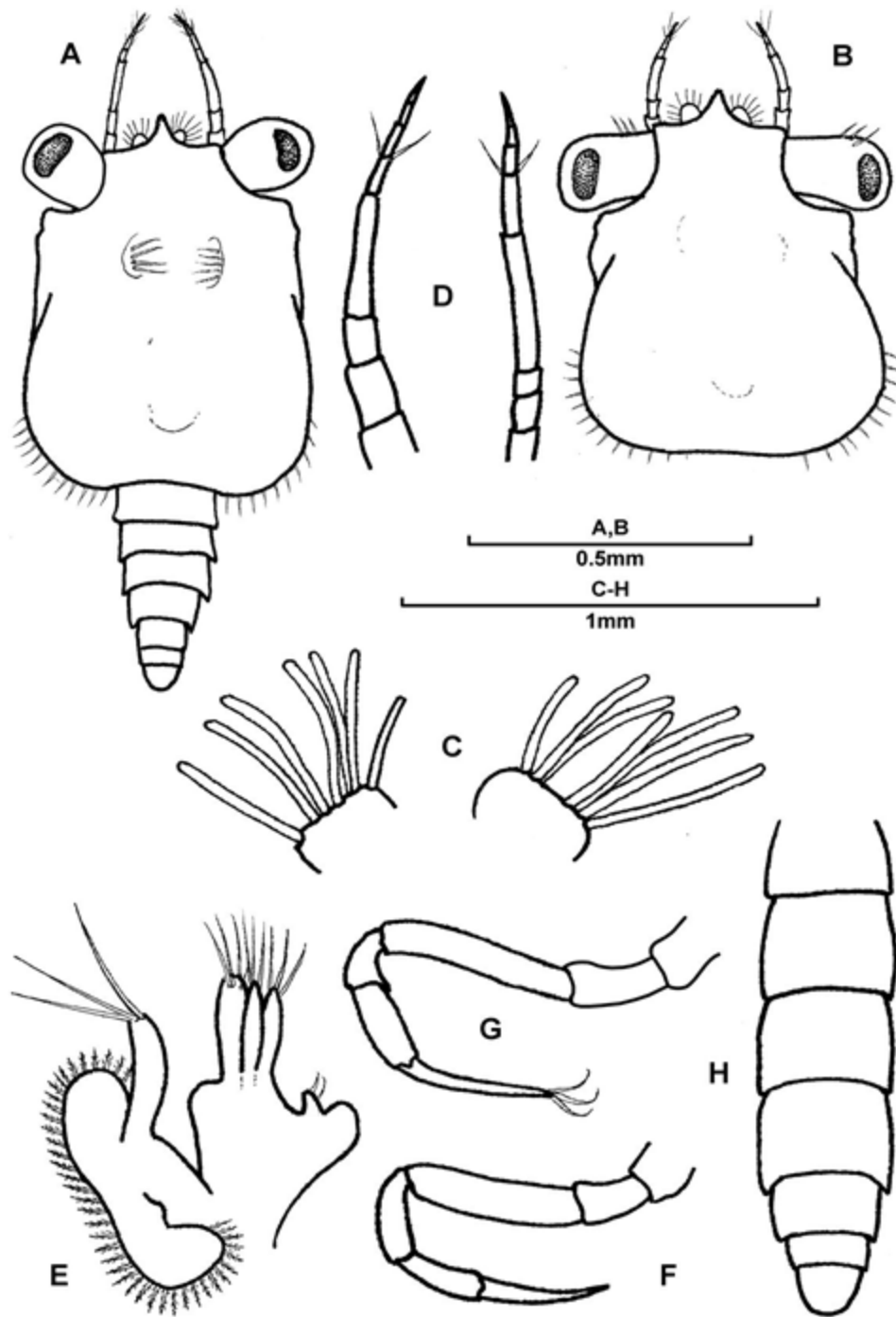


Figure 5. Taxonomy of megalopal stage of *Carcinus meanas* A) Dorsal view B) Carapace C) Antennules D) Antenna E) Maxilla F) Fourth pereopod G) Fifth pereopod H) Telson

The water temperature range (29-31°C), salinity (37-45‰), pH (7.8-8.0), DO (6.9-10.0 mg/L) and Transparency (40-120 cm) were measured during April to October 2018 (Table 1).

Table 1. Physico-chemical parameters and zooplankton samples were collected for taxonomic studies on megalopal stages of (Family-portunidae) from three designated sites of Indus deltaic area (Shahbandar, Ketibandar and Korangi creek) during April to October 2018.

Stations	Seasons	Months/Date of sample collection	Nos. of megalops collected in zooplankton sample	Water Temperature (°C)	Salinity (‰)	pH	Dissolved oxygen (mg/L)	Transparency (cm)
Shahbandar	Pre-monsoon	10-April-2018	09	29.6	42	7.8	9.6	120
	Monsoon	10-July-2018	04	30.2	45	7.8	10.0	90
	Post-Monsoon	15-October-2018	36	31.0	40	8.0	9.4	60
Ketibandar	Pre-monsoon	17-April-2018	23	29.0	33	8.0	7.1	90
	Monsoon	17-July-2018	18	31.0	30	8.0	9.0	70
	Post-Monsoon	29-October-2018	27	30.0	37	8.0	8.2	40
Korangi	Pre-monsoon	24-April-2018	13	30.0	39	8.0	6.9	40
	Monsoon	4-July-2018	24	29.5	38	8.0	7.0	60
	Post-Monsoon	18-October-2018	16	30.2	38	8.0	7.9	50

Discussion

The present study describes taxonomic features of three megalopal stages of *Portunus pelagicus* (Linnaeus, 1758), *Charybdis feriatus* (Linnaeus, 1758) and *Carcinus maenas* (Linnaeus, 1758) belonging to family Portunidae collected from Indus deltaic creek system. The present taxonomic studies on *P. pelagicus* were compared with Juwana et al. (1987) from Indonesia and Shinkarenko (1979) from Australian waters, Joisleen & Menon (2004) from southeast India. Based on taxonomic features carapace shape, antennae, antennae, mandibles, maxilla, first, second and third maxilla, pereopods, pleopods and telson were very similar to by Juwana et al. (1987).

Taxonomic studies on *Charybdis* sp. earlier reported by Ghory (2020) from Pakistan. The megalopa characteristics of *C. feriatus* were similar with Ghory (2020) on genus level. Campbell et al. (1984) described megalops of *C. feriatus* from Moreton Bay, Queensland. The taxonomic features of *C. feriatus* megalop, narrowing anteriorly, rostral plate shortened with a broad at exact angles and the present study shows the dorsal view of the carapace broadly triangular, the width is greater and narrows anteriorly to the rostral plate. Telson as long as wide, subsequent convex margin; Dorsal surface with one pair of small bristles. Current taxonomic studies of *C. feriatus* have been closely related to Campbell et al. (1984). No literature is available on the taxonomic features of *Carcinus maenas* species, thus, Spitzner et al. (2018), studied the organogenesis of the *Carcinus maenas*, presented the detailed atlas of the internal organization of the larva in a multi-method approach to complement obtainable descriptions of their external morphology. The present results indicate that the edges of the carapace may have curved and clumpy, the dorsal surface of the carapace is without distinct protuberances, the apex of the rostrum tapering forward or faintly descending, Platform among the eyes with a petty dejection. Based on these characteristics our specimen was like Spitzner et al. (2018). Weiss (2017) also examined the dorsal facade of the carapace with no divergent protuberances, edges and rostrum tips pointing slightly forward.

Acknowledgments

Authors would like to thank specially to Ms. Shumaila for her continuous help in analysing zooplankton samples and sorting of megalopal specimens. Authors would like to thanks to Mr. Abrar Ali, for his assistance in drawing illustrations and micro-photography. Also, we would like to express our thanks to Mr. Azizullah and Mr. Kashif Jameel for zooplankton samples collection, and special thanks to Marine Reference collection and Resource centre, for collection and laboratory facilities.

Conflict of Interest

The authors declare there is no conflict of interest in this study.

Author Contributions

All authors performed all the experiments and drafted the main manuscript text.

References

- Ali, Q. M., & Ahmed, Q. (2013). Composition of major zooplanktonic groups in Shahbunder creek system-indus deltaic area. *Pakistan Journal of Marine Sciences*, 22 (1&2), 43-59.
- Ali, Q. M., & Ahmed, Q. (2014). Distribution of major zooplankton groups in Ketibander creek system (Indus delta) during monsoon season, *Pakistan Journal of Marine Sciences*, 23 (1&2), 13-24.

- Bryars, S. R., & Havenhand, J. N. (2004). Temporal and spatial distribution and abundance of blue swimmer crab (*Portunus pelagicus*) larvae in a temperate gulf. *Marine and Freshwater Research*, 55: 809-818. <https://doi.org/10.1071/MF04045>.
- Campbell, G., Greenwood, J. G., & Fielder, D. R. (1984). The megalopa of *Charybdis feriata* (Linnaeus) with additions to the zoeal larvae descriptions (Decapoda, Portunidae). *Crustaceana*, 46(2), 160-165.
- Clark, P. F., & Paula, J. (2003). Descriptions of ten xanthoidean (Crustacea: Decapoda: Brachyura) first stage zoeas from Inhaca Island, Mozambique. *The Raffles Bulletin of Zoology*, 51(2), 323-378.
- Davie P. J. F. (2002). "Portunidae". Crustacea: Malacostraca: Eucarida (Part 2), Decapoda: Anomura, Brachyura. Volume 19 of Zoological catalogue of Australia, Australia. CSIRO Publishing. pp. 442–446. ISBN 978-0-643-05677-0.
- Ghory F. S., & Siddiqui F. A. (2000). The complete larval development of *Pilumnus* sp. (Decapoda: Brachyura: Pilumnidae) reared under laboratory conditions. *Proceedings of National Symposium on Arabian Sea as a Resource of Biological Diversity*, 207-227.
- Ghory, F. S., & Siddiqui, F. A. (2002). Occurrence and abundance of brachyuran larvae in the Manora Channel (Karachi, Pakistan) during 1993. *Pakistan Journal of Marine Sciences*, 11 (1&2), 27-36.
- Ghory, F. S., & Siddiqui, F. A. (2006). Percentage composition of different brachyuran larvae collected during 1994 in Manora Channel (Karachi, Pakistan). *Pakistan Journal of Marine Sciences*, 15 (1), 119-130.
- Ghory, F. S., & Siddiqui, F. A. (2008). Description of Leucosiidae (Crustacea: Brachyura) larval stages collected from the Manora Channel, Pakistan, during 1993-1995. *Pakistan Journal of Zoology*, 40 (5), 353-363.
- Ghory, F.S., Kazmi, Q. B., & Siddiqui, F. (2018). Redescription of the complete developmental stages of *Pilumnopus convexus* (Maccagno, 1936) (described as *Pilumnus* sp.) (Crustacea: Decapoda: Brachyura: Pilumnidae), *International Journal of Fauna and Biological Studies*, 5 (3): 193-202.
- Ghory, F.S. (2020). Morpho-taxonomic study of some planktonic caught megalopal stages collected from northern Arabian Sea. *Arthropoda*, 9 (4), 139-154.
- Hashmi, S. S. (1969). Studies on larval Ocypodidae (Macrophthalmus) hatched in the laboratory (Decapoda: Crustacea). *Pakistan Journal of Science and Research*, 21, 42-54.

- Hashmi, S. S. (1970a). The larvae of Elamena (Hymenosomidae) and Pinnotheres (Pinnotheridae) hatched in the laboratory (Decapoda: Crustacea). *Pakistan Journal of Scientific and Industrial Research*, 12: 212-278.
- Hashmi, S. S. (1970b). The brachyuran larvae of west Pakistan hatched in the laboratory (Decapoda:Crustacea). *Pakistan Journal of Zoology*, 2 (1): 81-93.
- Hines, A. H. (1986). Larval patterns in the life histories of brachyuran crabs (Crustacea, Decapoda, Brachyura), *Bulletin of Marine Science*, 39 (2), 444-466.
- Huang, Y.H. & Shih, H.T. (2021). Diversity in the Taiwanese swimming crabs (Crustacea: Brachyura: Portunidae) estimated through DNA Barcodes, with descriptions of 14 new records. *Zoological Studies*, 60, 1-45. <https://doi.org/10.6620/ZS.2021.60-60>.
- Josileen, J. & Menon, N. J. (2004). Larval stages of the blue swimmer crab, *Portunus pelagicus* (Linnaeus, 1758) (decapoda, brachyura). *Crustaceana*, 77 (7): 785-803.
- Juwana, S., Aswandy, I., & Pangabea, M. L. (1987). Larval development of the Indonesian blue swimming crab, *Portunus pelagicus* (L) (Crustacea: Decapoda: Portunidae) reared in the laboratory. *Marine Research in Indonesia*, 26(1), 29-49. <https://doi.org/10.14203/mri.v26i1.406>.
- Kailola, P. J., Williams, M. J., Stewart, P. C., Reichelt, R. E., Mcnee, A., & Grieve, C. (1993). Australian fisheries resources. Bureau of Resource Sciences, Department of Primary Industries and Energy, and the Fisheries Research and Development Corporation, Canberra, Australia.
- Kalhor, M. A., Tang, D., Jun, Y. H., Evgeny, M., Wang, S., & Buzdar, M. A. (2018). Fishery Appraisal of *Portunus* spp. (Family Portunidae) using Different Surplus Production Models from Pakistani Waters, Northern Arabian Sea, *Pakistan Journal of Zoology*, 50 (1), 135-141. <http://dx.doi.org/10.17582/journal.pjz/2018.50.1.135.141>.
- Kazmi, Q. B. (2003). Taxonomic studies of Crustaceans in Pakistan. Global Taxonomy Initiative in Asia. Report and Proc. 1st GIT Regional Workshop in Asia Putrajaya, Malaysia. (J. Shimura, Ed.). Natl. Inst. Environ. Studies, Japan No.175: 230-248.
- Korneiko, E. S., & Korn, O. M. (2009). Illustrated key for the identification of brachyuran zoeal stages (Crustacea: Decapoda) in the plankton of Peter the Great Bay (Sea of Japan). *Journal of the Marine Biological Association of the UK*, 89 (02), 379-386. <http://dx.doi.org/10.1017/S0025315408002762>.

- Newell, G. E. & Newell, R. C. (1977). *Marine Plankton a Practical guide*. 5th Ed. Hutchinson & Co. (Publishers) Ltd. 244 p.
- Pessani, D., Tirelli, T., & Flagella, S. (2004). Key for the identification of Mediterranean brachyuran megalopae. *Mediterranean Marine Science*, 5 (2), 53-64. <https://doi.org/10.12681/mms.203>.
- Potter, I. C., Chrystal, P. J., & Loneragan, N. R. (1983). The biology of the blue manna crab *P. pelagicus* in an Australian estuary. *Marine Biology*, 78, 75-85. <https://doi.org/10.1007/BF00392974>.
- Shinkarenko, L. (1979). Development of the larval stages of the blue swimming crab *Portunus pelagicus* L. (Portunidae : Decapoda : Crustacea). *Australian Journal of Marine and Freshwater Research*, 30, 485 – 503.
- Siddiqui, F. A., & Tirmizi, N. M. (1992). The complete larval development, including the first crab stage of *Pilumnus kampi* Deb, 1987 (Crustacea: Decapoda: Brachyura: Pilumnidae) reared in the laboratory. *Raffles Bulletin of Zoology*. 40 (2): 229- 244.
- Spitzner, F., Meth, R., Krüger, C., Nischik, E., Eiler, S., Sombke, A., Torres, G., & Harzsch, S. (2018). An atlas of larval organogenesis in the European shore crab *Carcinus maenas* L. (Decapoda, Brachyura, Portunidae), *Frontiers in Zoology*, 15 (27). <https://doi.org/10.1186/s12983-018-0271-z>.
- Stephenson, W. (1962). Evolution and ecology of portunid crabs, with special reference to Australian species. In: G.W. Leeper (Ed.) *The evolution of living organisms*, Melbourne University Press, Melbourne, pp. 311-327.
- Tirmizi, N. M., Siddiqui F. A., & Amir, N. (1993). Distribution of brachyuran larvae collected by R.V. Dr. Fridtjof Nansen, 1977 (Cruises 1, 2) from coastal waters of Pakistan. In: (Ed.) N.M. Tirmizi and Q.B. Kazmi *Proceedings of National Seminar on Study and Management in Coastal Zones in Pakistan*. MRC and UNESCO, Karachi : 181-188
- Weiss, H. M. (2017). Keys to the larvae of common decapods crustaceans (Lobsters, crabs and shrimps), in long Isanld sound, Project, Connecticut Sea Grant University of Connecticut, 48p.